



ISSUE 1/2018

Title Story // 3D Meta Models for Predictive Maintenance of Aircraft Engines

Particle Simulation

Engineering E-Motors

Simulation of Burst Protection

Design Optimization of a Wind Turbine for a Rowing Boat

Statistical Approach to Predict Sealing Performance

RDO-JOURNAL

optiSLang

SoS

**INFORM
NOW AND
APPLY**
FOR THE NEXT
CLASSES



Upgrade your work, upgrade your life.

The career-integrated study programs enable engineers with bachelor's and master's degrees to obtain scientifically based and practice-oriented simulation knowledge.

+	+	+	Applied Computational Mechanics	Computational Fluid Dynamics	Computational Medical Engineering
+	+	+	Responsible Universities	Responsible University	Responsible University
+	+	+	<ul style="list-style-type: none"> • HAW Landshut and Technische Hochschule Ingolstadt, Germany • PES University, India 	<ul style="list-style-type: none"> • HSR Hochschule für Technik Rapperswil, Switzerland 	<ul style="list-style-type: none"> • Witten/Herdecke University, Germany
+	+	+	Advancement Opportunities	Advancement Opportunities	Advancement Opportunities
+	+	+	<ul style="list-style-type: none"> • Master of Engineering (M.Eng.) • Qualification in selected modules 	<ul style="list-style-type: none"> • Certificate of Advanced Studies • Qualification in selected modules 	<ul style="list-style-type: none"> • Certificate of Advanced Studies • Qualification in selected modules
+	+	+	Module Offer (excerpt)	Module Offer	Module Offer
+	+	+	<ul style="list-style-type: none"> • Nonlinear and Contact Analysis • Materials and Material Models • Computational Dynamics • Fatigue and Fracture Mechanics • Modeling Techniques • Optimization and Robust Design 	<ul style="list-style-type: none"> • CFD in Practice • Fluid Dynamics and Heat Transfer • Mathematics and Computational Methods 	<ul style="list-style-type: none"> • Medical Fundamentals for Engineers • Regulatory Affairs for Development of Medical Devices • Biomechanical Simulation

3D META MODELS FOR PREDICTIVE MAINTENANCE OF AIRCRAFT ENGINES

Digital twins are one of the promising prospects for improved product lifecycles regarding Industry 4.0 scenarios. The resulting options for predictive maintenance of high-quality industrial goods create a lot of value added potential.

Dealing with durable products, such as aircraft engines, the challenge is to ensure high availability and reliable operation as well as to minimize maintenance and associated downtime. Maintenance, repair and overhaul (MRO) service providers bear a significant amount of risk when they have to calculate the total maintenance costs. To remain competitive, MRO providers need to develop predictive digital twins that are capable of indicating the expected maintenance costs based on specific operating conditions.

The fatigue behavior of aircraft engines is determined by regular loading, e.g. operating, starting and stopping of the engines, as well as by irregular damage of critical components, e.g. by bird strike on turbine blades. In addition, the number and duration of flights strongly varies between different airlines.

In order to increase the predictive capability and the value added of digital twins, a linking of sensor data and detailed physical models, e.g. high fidelity CAE simulation models, becomes necessary.

Detailed simulation models, which represent the processes of physical loads, allow in principle to predict the lifetime of components. Due to the high computational effort, however, constant updates of the actual performance data in daily fleet management as well as an integration into digital twins are not practicable. The main goal of the case study presented in the title story was therefore to develop real-time simulation workflows using 3D field meta-models. Here, the lifetime analyses of a turbine blade was chosen as an exemplary case.

Data-based Reduced Order Models (ROM), derived from 2D or 3D field analyses, provide both the required accuracy and processing speed. The Dynardo software Statistics on Structures and optiSLang were applied for the identification and generation of such Field Metamodels of Optimal Prognosis (FMOP). For the workflow integration of all existing data and knowledge regarding the fatigue behavior of the turbine blades, an optiSLang process setup was generated, which enters a representative parameter set of current flight data into the simulation models. This procedure provides the environment for an automated execution of simulation sets.

Apart from that, we again have selected case studies and customer stories concerning CAE-based Robust Design Optimization (RDO) applied in different industries.

I hope you will enjoy reading our magazine.

Yours sincerely



Johannes Will
Managing Director DYNARDO GmbH

Weimar, June 2018

CONTENT

2 // TITLE STORY // FIELD META MODELS

Real-time processing with 3D meta models for predictive maintenance of aircraft engines

8 // CASE STUDY // PROCESS ENGINEERING

Calibration of angle-of-repose and draw-down angle using a ROCKY-DEM simulation

12 // CUSTOMER STORY // AUTOMOTIVE ENGINEERING

Engineering e-motors

16 // CASE STUDY // CIVIL ENGINEERING

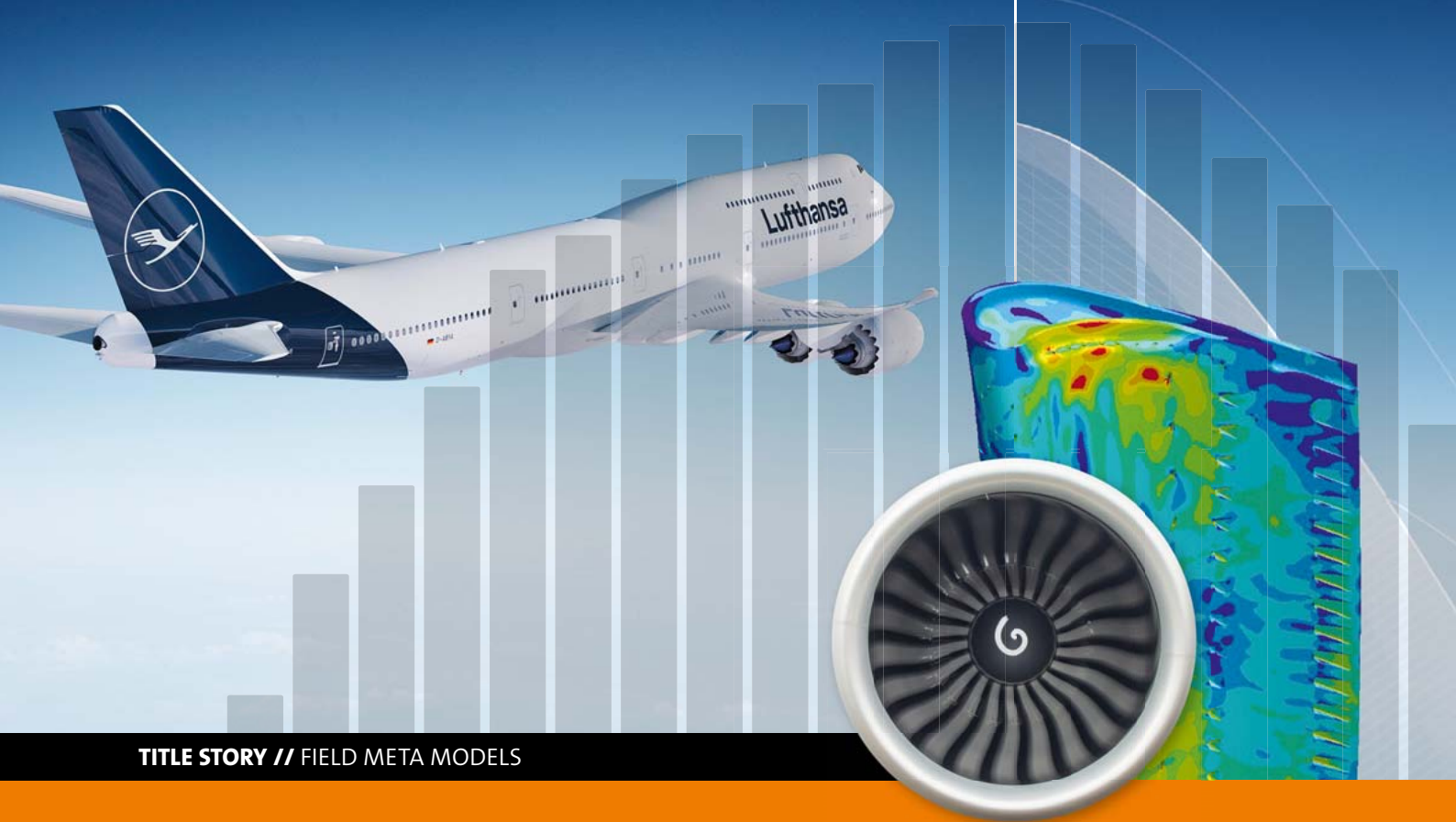
Simulation of burst protection with ANSYS LS-DYNA and optiSLang

20 // CUSTOMER STORY // MECHANICAL ENGINEERING

Design optimization of a wind turbine for the rowing boat "AKROS"

24 // CUSTOMER STORY // AUTOMOTIVE ENGINEERING

Statistical approach to predict sealing performance



TITLE STORY // FIELD META MODELS

REAL-TIME PROCESSING WITH 3D META MODELS FOR PREDICTIVE MAINTENANCE OF AIRCRAFT ENGINES

At Lufthansa Technik (LHT), field meta models efficiently enable the life prediction of components, such as a turbine blade, taking into consideration the specific operating conditions.

Introduction

LHT, as a part of the Lufthansa Group, is an independent provider of maintenance, repair and overhaul (MRO) services in the world's airline business. Organized in different product divisions, LHT offers aircraft services for line and base maintenance including overhaul, component services, landing gear services, VIP & special mission aircraft services, as well as engine services. In the product division of engine services, different offerings are made to different types of customers. Other MRO providers may procure only individual engine part repairs, while engine manufacturers may contract individual engine overhauls to be performed in an LHT engine shop. Airlines, however, will usually require MRO coverage for their whole fleet, including engineering tasks, such as maintenance planning and workscope definition. In addition to engine maintenance performed in the shop, LHT also offers Mobile Engine Services, which are carried out while the engine is still on-wing, often with the aim of avoiding an imminent engine removal.

Motivation for the use of prognostic methods for predictive maintenance

The engine is one of the most complex and technologically

challenging components of an aircraft. They usually account for a significant portion of any airline's total operating cost. Furthermore, as shown in Fig. 1 for the engine type CF6-80C2, the largest portion of the total cost, produced during an engine's life cycle, does not stem from the engine's purchase, but from the MRO expenses. In the last 30 years, this has led to a very competitive market for engine MRO, with engine manufacturers stepping into the aftermarket besides the established independent MRO providers. As in all competitive markets, the margin for error in assessing the risks involved with a certain contract tends to be low.

Contracts for the MRO coverage of a whole engine fleet are usually rather long-term (10 – 15 years run-time are no exception). These types of contracts are very complex. They increasingly tend to contain fixed price elements, price caps or they can be right-out flat-rate contracts. Either way, the contract structure has two significant implications for the MRO provider:

1. Because of the price caps and/or fixed price elements, the maintenance provider carries a significant portion of the risk involved in the prediction of the total maintenance cost.

- Because of the long run-time, predictions for expected total maintenance cost have to be made far into the future and, at the same time, they have to be very accurate in order to produce a competitive offer.

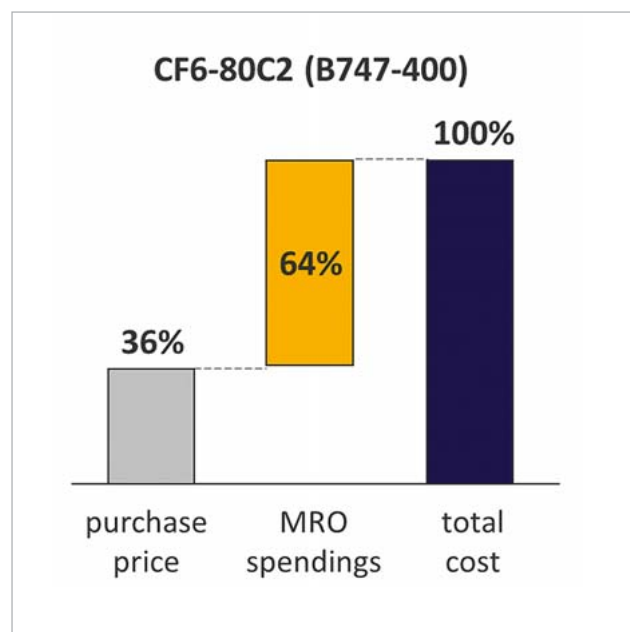


Fig. 1: Engine lifetime cost

The different factors mentioned above make it necessary for MRO providers to develop methods capable of accurately predicting the expected maintenance cost as a function of a customer's specific operating conditions in order to be competitive. It is no longer sufficient to disassemble and assemble engines efficiently in a shop, nor to perform any number of engine part repairs. In addition to this, it is increasingly important to perform proper fleet management throughout the operation. This involves removal and maintenance planning in a manner that allows constant monitoring. Once a plan was made, it has to be compared to the actual performance of an engine fleet, and the predictions for further development have to be constantly updated. If done properly, this will allow risk management through the early detection of problems, and will thus reduce the engine maintenance cost per flight hour.

Removal and maintenance planning requires the ability to predict how the engines will behave when exposed to certain operating conditions over several years. The engine behavior in this context consists of both the overall performance deterioration, as usually measured through the exhaust gas temperature margin (EGT Margin), and the damage to critical components, such as turbine blades, which may tend to suffer cracks at certain locations. In Fig. 2, a CFM56-5C high pressure turbine blade is shown as an example. This blade usually develops cracks at the root trailing edge (marked location). An engine removal is required if these cracks reach a critical length. The number of flights or cycles to reach this point and, thus, the achievable time

on wing, varies from airline to airline. It is depending on the specific operating conditions that the engines are exposed to. The major aim of the research presented here is to develop a method for predicting the useful life of components, such as a turbine blade, taking into consideration the specific operating conditions.

Big data reaching its limits

How can such a matter best be approached? The issue is complex and highly non-linear, and there are many parameters involved. The current "state-of-the-art" would likely call for a big data analysis based on all available fleet and

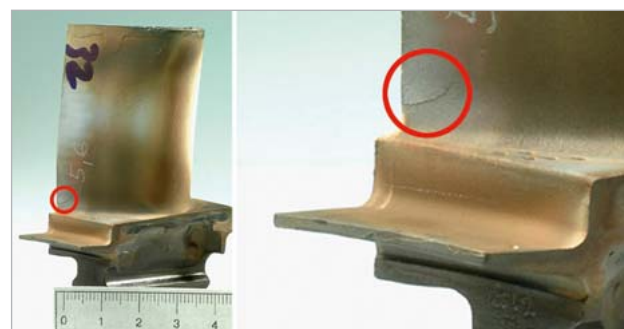


Fig. 2: Engine blade with crack on trailing edge (red circle)

operational data, with statistical methods identifying sensitivities that can be used as surrogate models to predict loading and resulting life for critical engine components.

LHT experience shows that a high amount of parameters influencing the results makes it all but impossible to derive meaningful results from such an analysis unless the data is filtered properly. However, then the amount of comparable data points is usually insufficient for a meaningful statistical analysis. Furthermore, while statistical methods or neuronal networks may provide a result, they usually work as black boxes and do not provide any understanding of the sensitivities. Consequently, this makes it impossible to assess if the model is working properly or not, especially when being used for extrapolations. Therefore, LHT investigates the approach of combining available fleet and operational data to extract statistical models for engine component loading. In this step, filtering and decomposition strategies become crucial to derive meaningful results. In addition, LHT uses high fidelity CAE models to predict the engine part loading and life.

A detailed CAE-based model as base to predict loading and life

LHT has been engaged for several years in the development of physics-based engine models. These include thermodynamic cycle models of the engine as a whole, as well as models for numerical simulation (CFD, FEM) of individual modules and components. Physics-based models usually

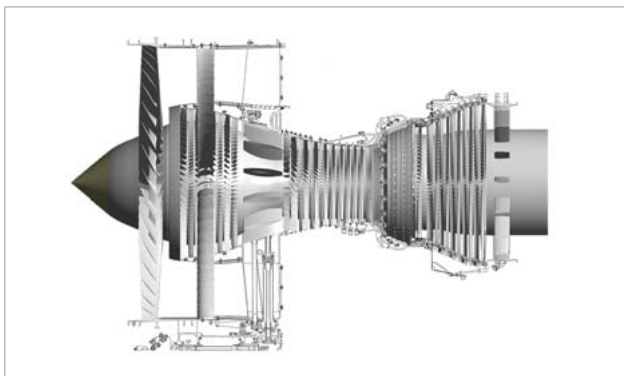


Fig. 3: Geometry of a CFM56-5C engine

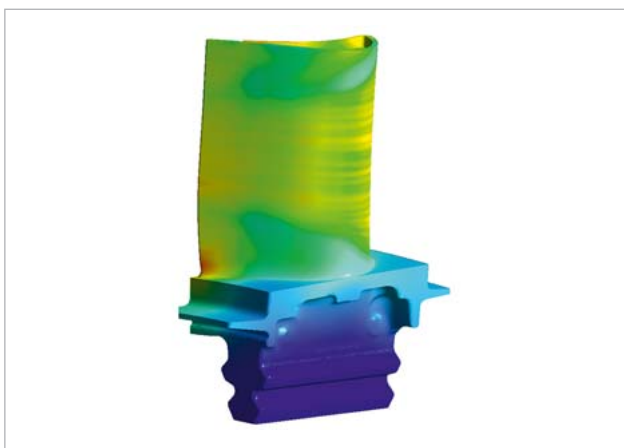


Fig. 4: Temperatures on a high-pressure turbine blade

include an accurate representation of the engine's geometry (Fig. 3 shows the geometry model of the CFM56-5C) and the engine's behavior. They also make it possible to determine the loads in a certain component under actual operating conditions. As an example, Fig. 4 shows a temperature distribution at take-off for the same turbine blade as shown in Fig. 2. With this information, useful predictions about life of critical components become possible.

The drawback of this modeling approach is the high computational cost caused by high fidelity simulations. A faster solution is needed in a fleet management framework with the requirement of constant updates of removal planning based on actual performance data. Therefore, surrogate models were established, which operate quickly and keep a high quality in terms of the result accuracy. The challenge for these surrogate models is that not only scalar non-linear responses need to be taken into account. The surrogate models need to forecast field responses, like stress distribution throughout the blade.

Field surrogate modeling approach (FMOP)

Based on this need for accurate field surrogate models, Lufthansa Technik, ITB and Dynardo teamed up for the development of a highly adaptive workflow providing the utmost possible automatized generation of field surrogate

models. For generating the field surrogate models, the Dynardo technology to identify Field Metamodels of Optimal Prognosis (FMOP) was used. This was done for the HPT-Blade mentioned before and aims to be applied on a vast amount of engine components.

The core idea of this project is to combine all the existing data and knowledge about the engine fatigue into one workflow. This includes the flight data, as well as joining existing simulation models in a one-way fluid-structure interaction (FSI). Here, an optiSLang setup manages the process, feeding a representative set of the gathered flight data into the simulation models and providing the environment for the automated execution of the set of simulations. When all design points are calculated, the workflow is finished with an instance of Statistics on Structures, which automatically generates and exports field surrogate models for the results of the FSI simulation. This surrogate model may then be used to rapidly approximate the responses of the structure for an infinite amount of operation points or can be used for further investigations.

Numerical challenges

While the setup in optiSLang is easily accessible (see Fig. 5), a big part of the challenge in this collaboration was the efficient management and connection of the fluid-structure interaction and its highly detailed numerical models. To put this into perspective, some metrics of the numerical models have to be brought to mind. Even though the mechanical utilization is what shall be approximated by the surrogate model, the variable loads used as input data consist of flight operation parameters, i.e. in detail measured values from the engine. This includes values, such as temperatures, pressures and number of revolutions. Consequently, the loads (pressures and temperatures) for the final mechanical simulations have to be derived from the results of the fluid simulation.

The model of the high pressure part of the engine contains more than just the high-pressure blade of interest. Additional stages and their respective vanes have to be considered in order to obtain a precise answer of the system for any given operation point. Fig. 5 shows the solid domains (blue) used in the fluid simulation, which are surrounded by the fluid itself. Inner cooling channels of the HPT blade are also considered.

This results in a tremendous mesh with about 80 million nodes. These mesh sizes cause a great need for computational power in order to calculate the necessary number of design points to generate the field surrogate models in an acceptable amount of time. While this of course can be solved by simply using simultaneous design execution on powerful hardware, the additional cost for hardware and software licensing limits the achievable speed-up. Additional initial engineering effort on the setup quickly pays off and scales by each design point. For example, the fluid simulation was speeded up only by a tight definition of convergence criteria for the temperatures and pressures

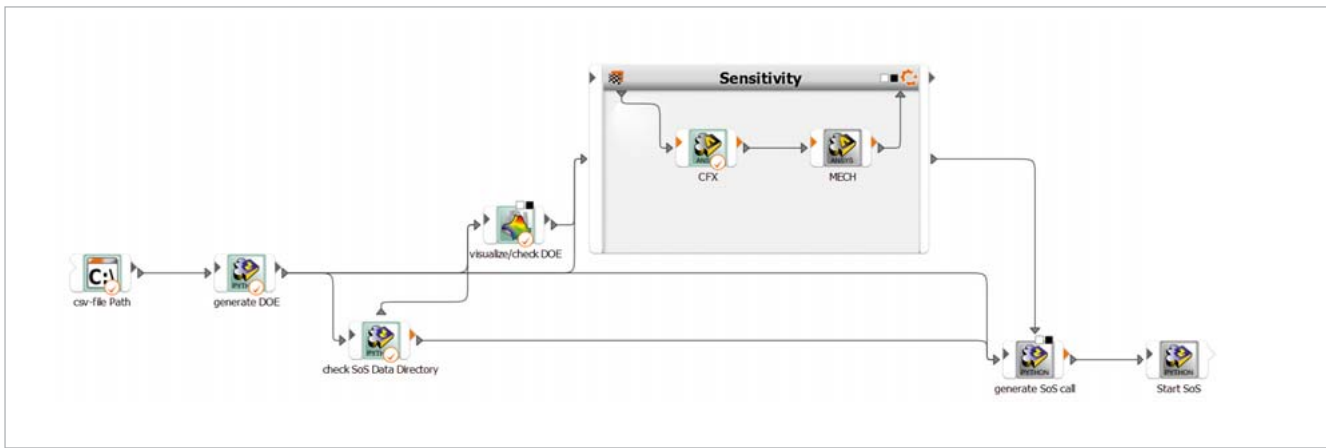


Fig. 5: optiSLang workflow

around the HPT-Blade. Furthermore, with an automatized selection of the most appropriate initial solution for each design point, the solution time was reduced to about 15 hours per design point on a 128 core cluster.

Only about one hour of computation time was used for the mechanical simulation. The involved geometries are approximated by a rather small node number of 6 million as shown in Fig. 6.

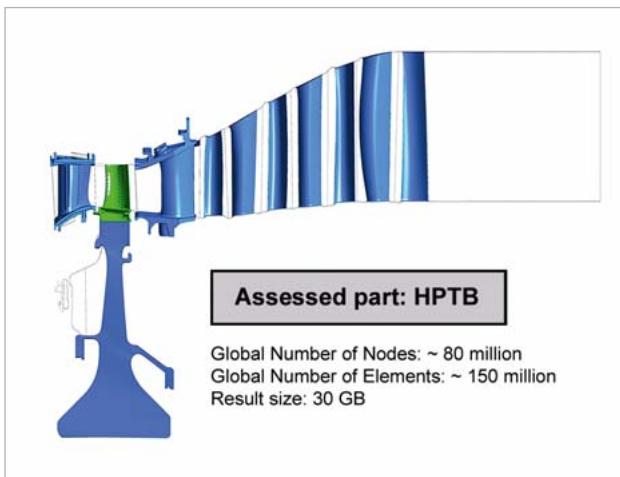


Fig. 6: Scope of the fluid simulation

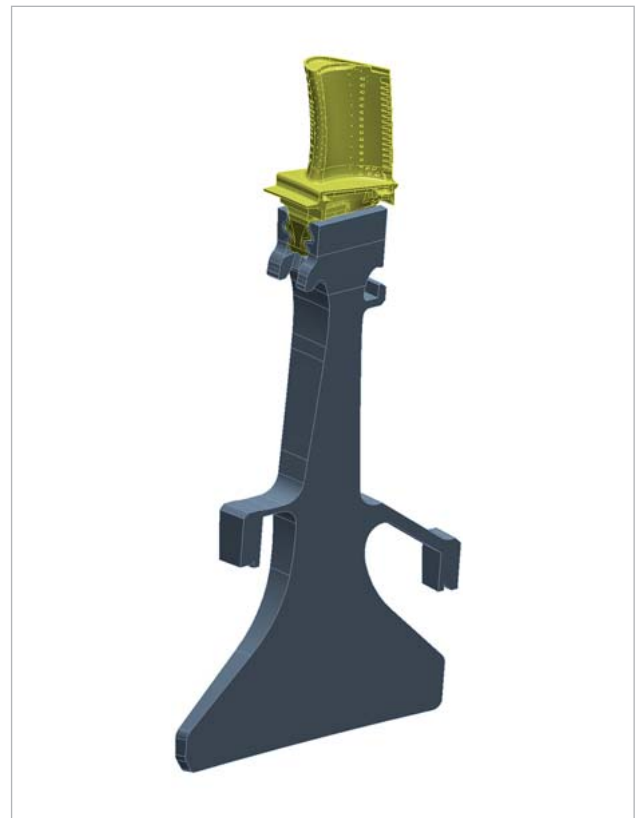


Fig. 7: FE model of the blade

Validating the results

In the end, for 50 design points the total runtime of the FSI added up to about a month of computation time and approximately 2 TB of data. This data was then fed into Statistics on Structures by the workflow, creating two output files. One containing just the field surrogate model for further use and the other containing additional result sets of validation design points. These validation design points were not used for the generation of the surrogate model but can be directly compared with the values approximated by the surrogate model in SoS. A comparison of FE-results, the results from the surrogate model (also referred to as Field Metamodel of Optimal prognosis – FMOP) and their relative deviation (result accuracy) is presented in Fig. 7.

Fig. 8 (see next page) shows a screenshot directly taken from SoS. As a highlight, the F-CoP [Total] (a measurement of the quality of prediction taking into account all input variability) of the temperatures reaches a value of 99 %, while responses like the principle stresses, which are highly sensible to meshing, and boundary conditions maintain a value of 91 % at worst.

Furthermore, sensitivities can directly be derived from the data, which allow quick identification of the most important input parameters. In this case, for most responses, variation of the boundary condition parameter T4soll shows the largest quantitative impact to most response variation (refer to F-COP [T4soll] at Fig.9, see next page).

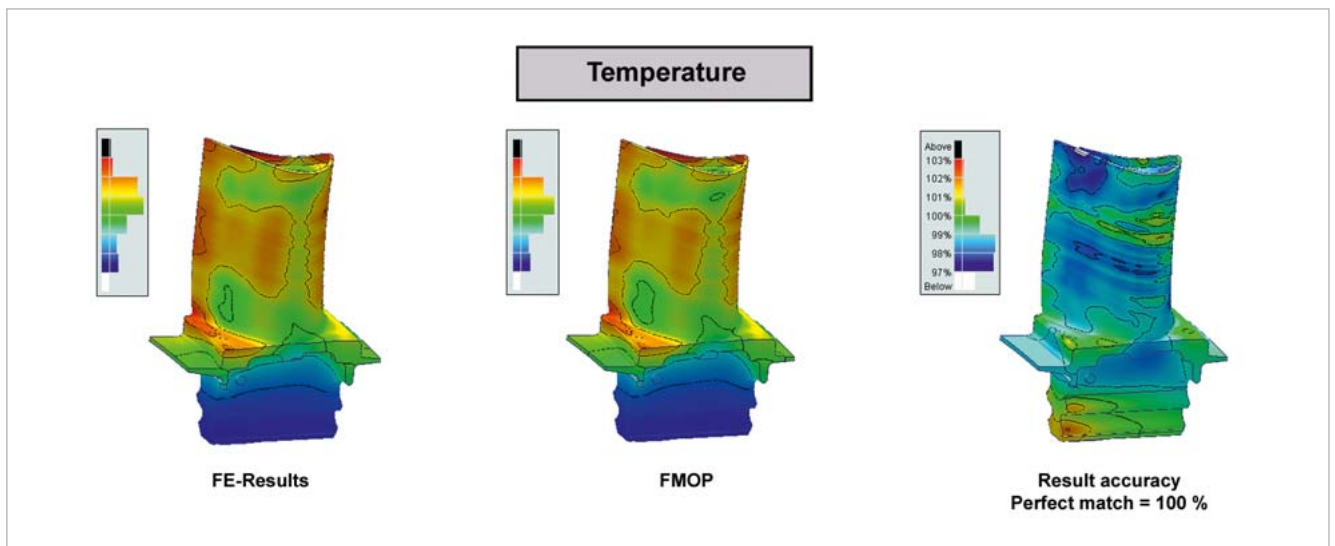


Fig. 8: Comparison of the calculated temperatures (left), the predicted temperatures (middle) and their accuracy (right)

	S1	S2	S3	SX	SXY	SXZ	SY	SYZ	SZ	TEMP
Capped_dif50_data										
F-CoP[Input_N1]	0.52 %	0.65 %	0.63 %	0.04 %	0.12 %	0.11 %	0.09 %	0.13 %	0.07 %	
F-CoP[Input_N2]	5.29 %	3.75 %	3.84 %	6.53 %	5.53 %	4.35 %	3.81 %	4.00 %	3.56 %	0.03 %
F-CoP[P25]	0.72 %	1.01 %	0.95 %	0.13 %	0.24 %	0.24 %	0.25 %	0.30 %	0.20 %	
F-CoP[P3]	1.53 %	2.89 %	2.28 %	5.46 %	5.48 %	5.40 %	5.41 %	5.51 %	4.86 %	0.20 %
#2 F-CoP[P4soll]	18.02 %	17.26 %	14.49 %	16.67 %	14.70 %	17.62 %	14.32 %	17.52 %	18.33 %	
F-CoP[P5Vorgabe]	1.65 %	1.58 %	1.43 %	0.06 %	0.19 %	0.20 %	0.17 %	0.18 %	0.15 %	
F-CoP[T25]	0.66 %	1.64 %	1.07 %	0.50 %	0.99 %	0.93 %	1.94 %	1.21 %	0.79 %	0.02 %
F-CoP[T3]	1.88 %	5.66 %	4.59 %	1.68 %	3.57 %	2.26 %	11.31 %	4.87 %	2.60 %	49.88 %
#1 F-CoP[T4soll]	82.83 %	64.32 %	62.67 %	78.36 %	70.11 %	72.26 %	56.74 %	63.67 %	64.44 %	49.02 %
F-CoP[Total]	95.37 %	91.52 %	91.96 %	96.49 %	92.38 %	93.27 %	92.00 %	92.08 %	95.01 %	99.21 %
mean[FMOP]										
sigma[FMOP]										

Fig. 9: Screenshot from Statistics on Structures showing the correlation between input and output parameters

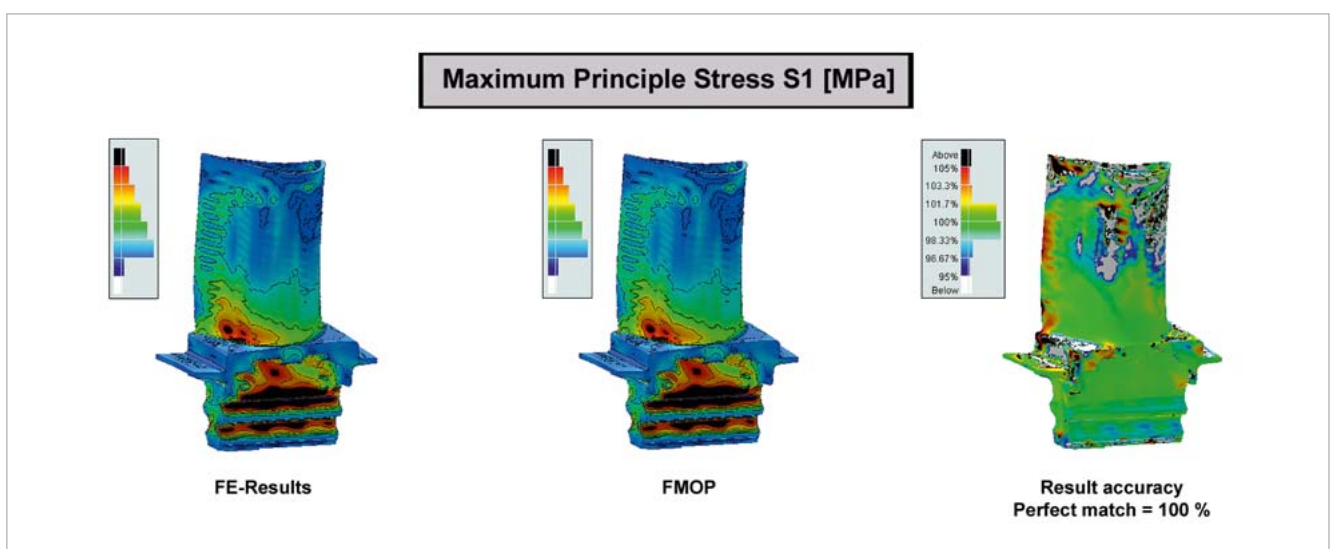


Fig. 10: Comparison of the calculated maximum principle stresses S1 (left), the predicted S1 (middle) and their accuracy (right)

Similar to the temperature results shown in Fig. 7, the maximum principle stress is compared in Fig. 9.

Since finally the behavior of the blade regarding fatigue is of interest, the percental result accuracy of the stresses is not directly correlated with the accuracy of the fatigue and the derived prediction of lifetime.

As shown in Fig. 10, the local accuracy for predicting the principle stress may be off by 5 % and more. However, if the total stress level is considered, the areas of high stresses from the FE-result as well as from the FMOP do not overlap with the less accurate regions from the accuracy plot. Vice versa, the regions with an interesting high stress level show a satisfying high accuracy. For example, the stresses of the root trailing edge from Fig. 2, which tends to crack, is predicted with a rather small inaccuracy of about 3 %.

An evaluation of the generated field surrogate models quality considering the predicted lifetime yet has to be conducted. However, the workflow itself proves to be working and the initial comparisons using the validation points show promising results.

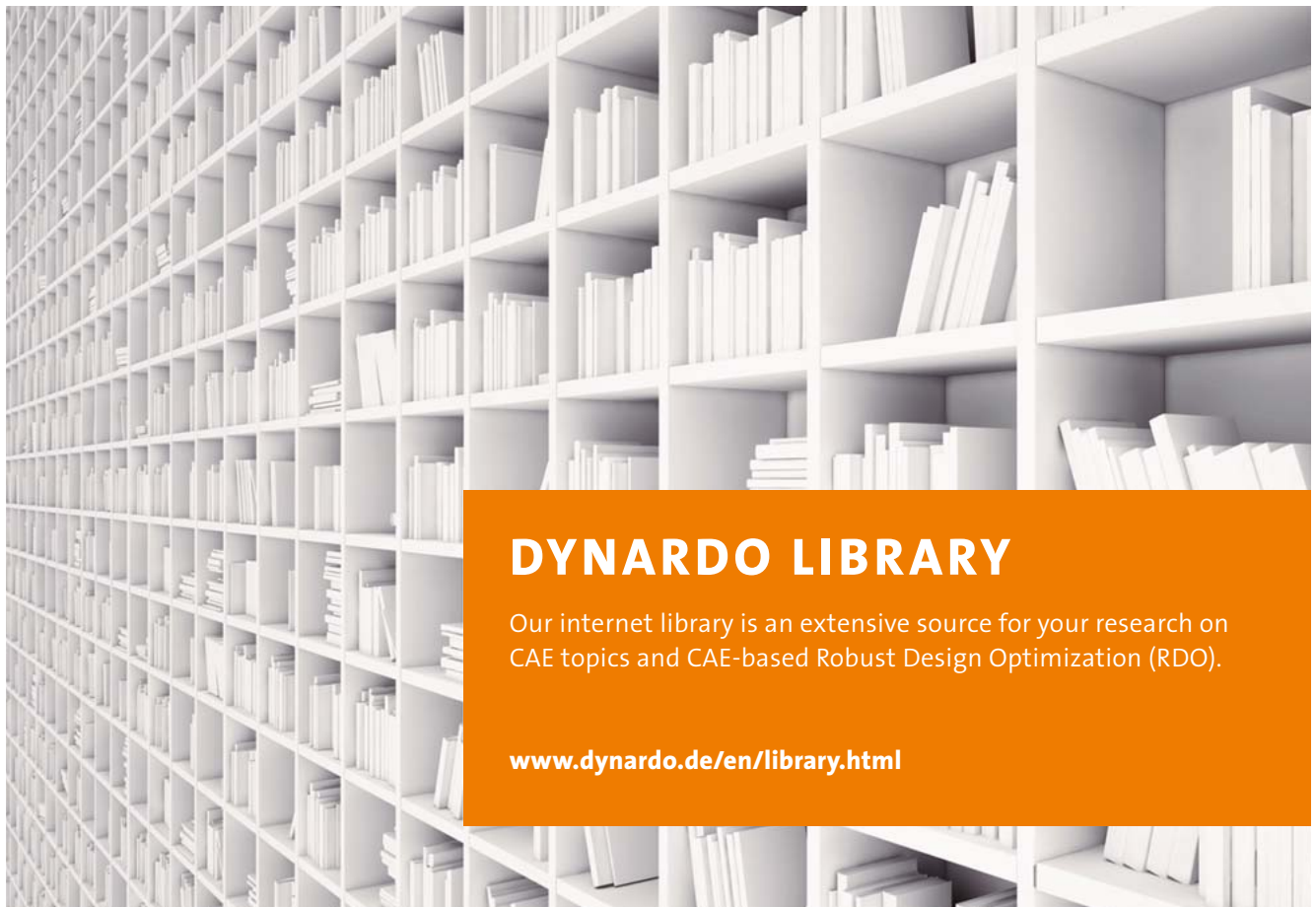
Applied on further engine components, this process leads to field surrogate models which will give very important information to digital twins for the critical parts in engine operation and may be the cutting-edge technology making precise predictive maintenance predictions possible.

Summary

This article presented a new approach for building field surrogate models for a real-time digital twin for predictive maintenance of aircraft engines. The simulation model is generated with ANSYS, the workflow is organized by optiSlang and the meta modeling is managed by SoS. The numerical models are very complex and require an HPC cluster for half a day for each single design calculation. The resulting field surrogate model is sufficiently accurate for predicting temperatures, stresses and strains and reduces the computing time to a few seconds.

Authors //

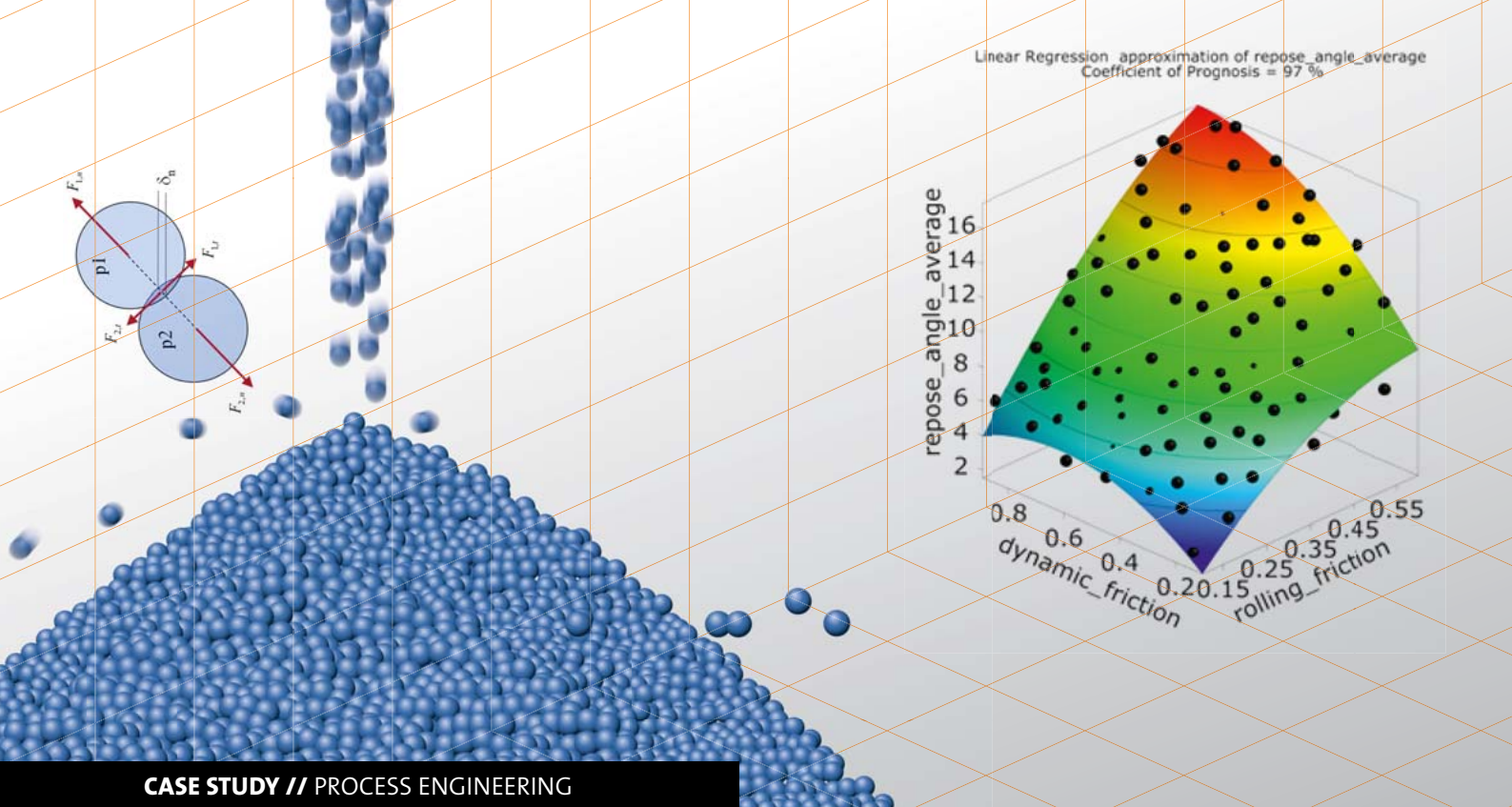
Holger Schulze-Spüntrup (ITB) / Christian Werner-Spatz, Marc Zschieschank (Lufthansa Technik) / Sebastian Wolff (DYNARDO Austria GmbH)



DYNARDO LIBRARY

Our internet library is an extensive source for your research on CAE topics and CAE-based Robust Design Optimization (RDO).

www.dynardo.de/en/library.html



CASE STUDY // PROCESS ENGINEERING

CALIBRATION OF ANGLE-OF-REPOSE AND DRAW-DOWN ANGLE USING A ROCKY-DEM SIMULATION

Rocky Discrete Element Method (DEM) and optiSlang were used to calibrate a model for the simulation of particle behavior in order to optimize the geometry of a bulk material funnel.

Motivation

The angle-of-repose and the draw-down angle are critical parameters for assessing the particle behavior, e.g. regarding bulk material. Prior to a particle simulation, the unknown properties and parameters of the numerical simulation should be determined by reproducing an experiment within a particle simulation.

Calibration represents the starting point of a parameter study, especially if uncertainties regarding the determination of material constants or the arrangement of constraints have to be considered in numerical simulation. Dealing with particle simulations, this is a constant challenge, because the individual properties depend not only on the material of the particle, but also on its shape and the environmental conditions. This results in a large amount of parameters, which make the identification of interactions significantly more difficult. A sensitivity study was first performed to generate the Metamodel of Optimal Prognosis (MOP) and to identify the important parameters. Such an approach is particularly important and challenging for the Discrete Element Method (DEM), because of the consideration of many parameters and the processing of quantities due to the noise of the numerical solution. These boundary

conditions require a variant study with an efficient investigation of the parameter space. In the procedure, meta-model algorithms are used to not simply “fit” the data, but also take into account the influence of solver noise and, thus, illustrate global trends. These requirements can be fulfilled by using the MOP approach.

The following example applies the fixed-funnel method to identify the parameters for describing the particles. The simulation process of this method is shown in Fig. 1. As soon



Fig. 1: Illustration of the transient simulation to determine the angle-of-repose and the draw-down angle of a bulk material

	Name	Parameter type	Reference value	Constant	Operation	Value type	Resolution	Range		Range plot
1	particle_density	Opt.+Stoch.	2750	<input type="checkbox"/>		REAL	Continuous	2700	2800	
2	static_friction	Dependent	0.6875	<input type="checkbox"/>	scaling_factor_friction*dynamic_friction					
3	dynamic_friction	Opt.+Stoch.	0.55	<input type="checkbox"/>		REAL	Continuous	0.4	0.6	
4	restitution	Opt.+Stoch.	0.55	<input type="checkbox"/>		REAL	Continuous	0.1	0.6	
5	rolling_friction	Opt.+Stoch.	0.55	<input type="checkbox"/>		REAL	Continuous	0.1	0.6	
6	mass_flow	Opt.+Stoch.	20	<input type="checkbox"/>		REAL	Continuous	19	21	
7	particle_diameter	Opt.+Stoch.	10	<input type="checkbox"/>		REAL	Continuous	9	11	
8	E_Modulus	Opt.+Stoch.	1e+07	<input type="checkbox"/>		REAL	Continuous	8e+06	1.2e+07	
9	scaling_factor_friction	Opt.+Stoch.	1.25	<input type="checkbox"/>		REAL	Continuous	1	1.5	

Fig. 2: Overview of the parameter and their corresponding ranges

as the cylinder is completely filled with particles, it is moved upwards creating the typical form of solid bulk. Here, both the angle-of-repose and the draw-down angle can be determined as a mean value along the bulk material heap.

The angle-of-repose represents the outer angle of the bulk material and can be determined directly after such an experiment. The draw-down angle describes the inner angle after the bulk heap has dispersed from the middle. The mean value along the bulk material was then calculated for both angles and the results were used in the subsequent analyses.

Procedure

The process of solving this task is divided into two steps. First, the conduction of a sensitivity analysis and, second, the use of an optimizer to minimize the deviations between the simulation model and the experiment.

Calibration

The aim of a calibration is to match the results of a simulation to the measurements. This can only be obtained after an identification of the important parameters. Once they are detected, a variation can be conducted to minimize the deviation. In this study, the physical properties were used as parameters and varied in the ranges shown in Fig. 2. It should always be noted here that some parameters cannot be considered as independent. In this case, the static and dynamic friction is multiplied by a weighting factor that describes the ratio between them and is always less than one. This value also represents a physical constraint in the parameter study. In addition, the particle density, the particle diameter and the mass flow while entering the test tube were examined.

The general procedure for a calibration is shown in Fig. 3. First, the important parameters should be identified. Af-

terwards a calibration between simulation and experiment can be achieved with these important parameters by means of an optimization algorithm.

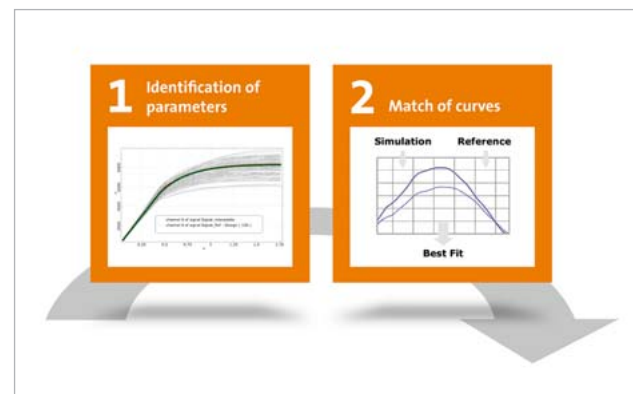


Fig. 3: General workflow of a calibration with, first, the identification and, second, the optimization of these found parameters to fit the simulation with the reference data

Workflow

Based on the obtained parameters, 100 simulations were generated arranged in a Latin Hypercube as part of a Design-of-Experiment. The parameters were transferred to Rocky DEM using the custom integration that is pre-installed in optiSLang. Then the model was updated and numerically solved. Fig. 4 (see next page) illustrates the workflow.

After completion of the simulation, the results were transferred back to optiSLang and used for the evaluation. Using these 100 simulations from the sensitivity study, the MOP could be created for the two result values draw-down angle and angle-of-repose. The MOP was then used for an optimization to minimize the deviations between simulation and experiment. The aim of the optimization was defined as

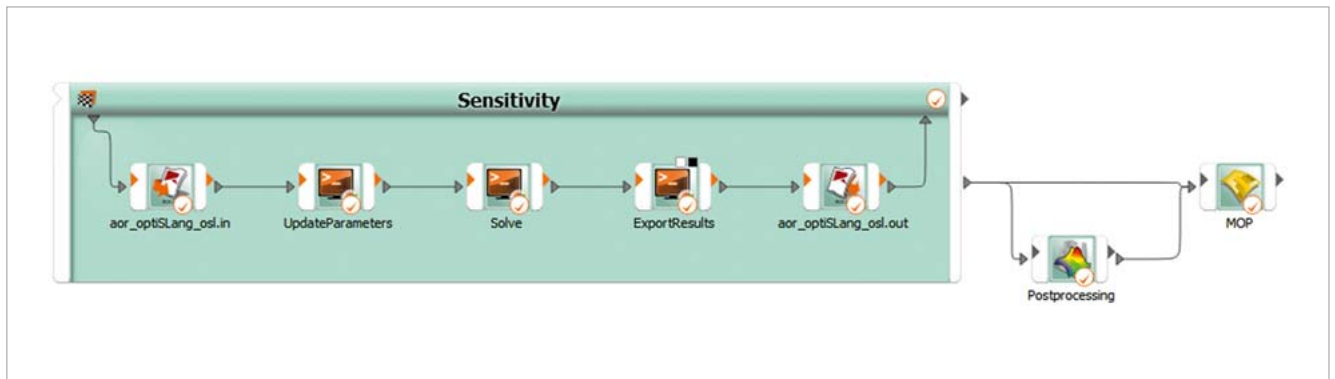


Fig. 4: optiSLang workflow of an automatized sensitivity study for a Rocky DEM simulation

the sum of the squared differences between simulation and experiment. Here, a Non-Linear Programming by Quadratic Lagrangian (NLPQL) proved to be a suitable method. This procedure yielded a sufficient calibration without using another numerical simulation run.

Results

Based on the results of the sensitivity study, first, the range of values of the result variables could be compared with the experimental data. The results and the associated experimental data are comparatively shown in Fig. 5. The experimental values are positioned in the middle of the result space surrounded by the simulation results. This indicates that the parameter space is sufficiently chosen and a calibration is possible. At this point, however, the optimum in the parameter space cannot yet be located. For this purpose, a reduction of the parameters and a subsequent optimization is required.

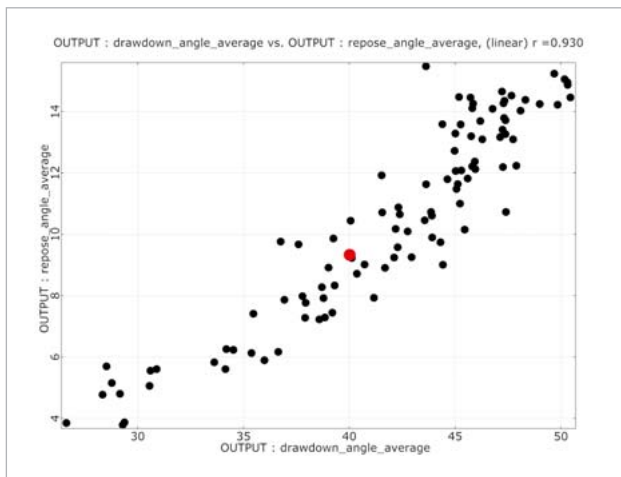


Fig. 5: Illustration of the experimental values (red), which are the calibration target and the results of the performed simulations

The reduction of the important parameters could be reached by using the MOP. Beside the identification of important parameters, the MOP also enables the elimination of the strong solver noise as a typical phenomenon in a DEM simulation.

For the data set examined here, the rolling friction is of importance, because it only describes the two result variables. With the help of the subsequent optimization based on the MOP, the rolling friction could be identified. Here, the deviation between simulation and experiment was minimal. Thus, both values were accurately determined, the angle-of-repose differs 0.21° from the experiment and the draw-down angle with 0.1°. This small remaining deviation can be seen exemplarily for the noise of the Rocky simulation in this example.

Conclusion

Using the created workflow, Rocky DEM simulations can be coupled with other platforms via optiSLang and optimizations can also be carried out. The procedure is fully automated and, thus, less prone to errors. The workflow was used to determine the numerical input variables based on experimental data for the simulation of the angle-of-repose and the draw-down angle. The identification of the rolling friction as an important parameter as well as a sufficient plausibility check including a physical test would not have been possible without an automated parameter study using the MOP. Those parameters identified as not important cannot be calibrated by the experiment. Such values have to be considered in other experiments.

By means of optimization, the suitable rolling friction could be determined. For this purpose, not only the values of the MOP but also the values of the numerical model were calculated. The deviation between them is just a few percent, thus, this value of rolling friction could be used for further simulations.

Author//

Bernd Büttner (Dynardo GmbH)

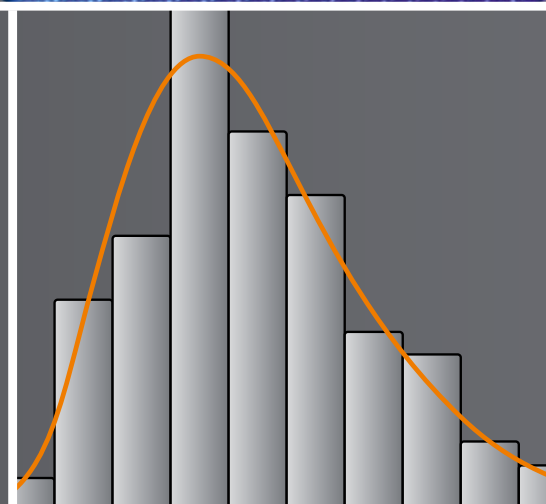
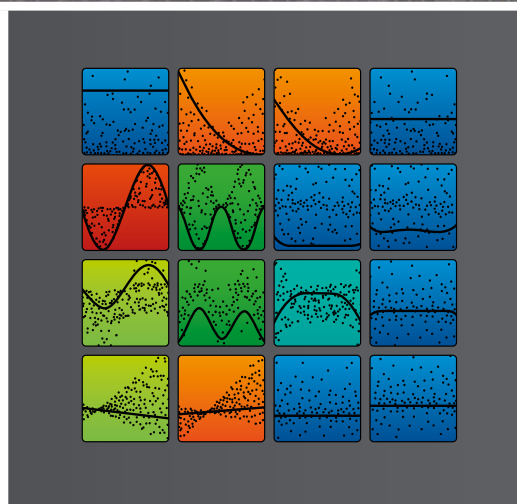
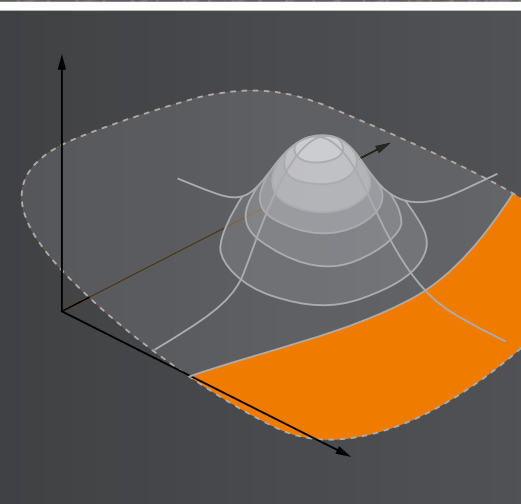
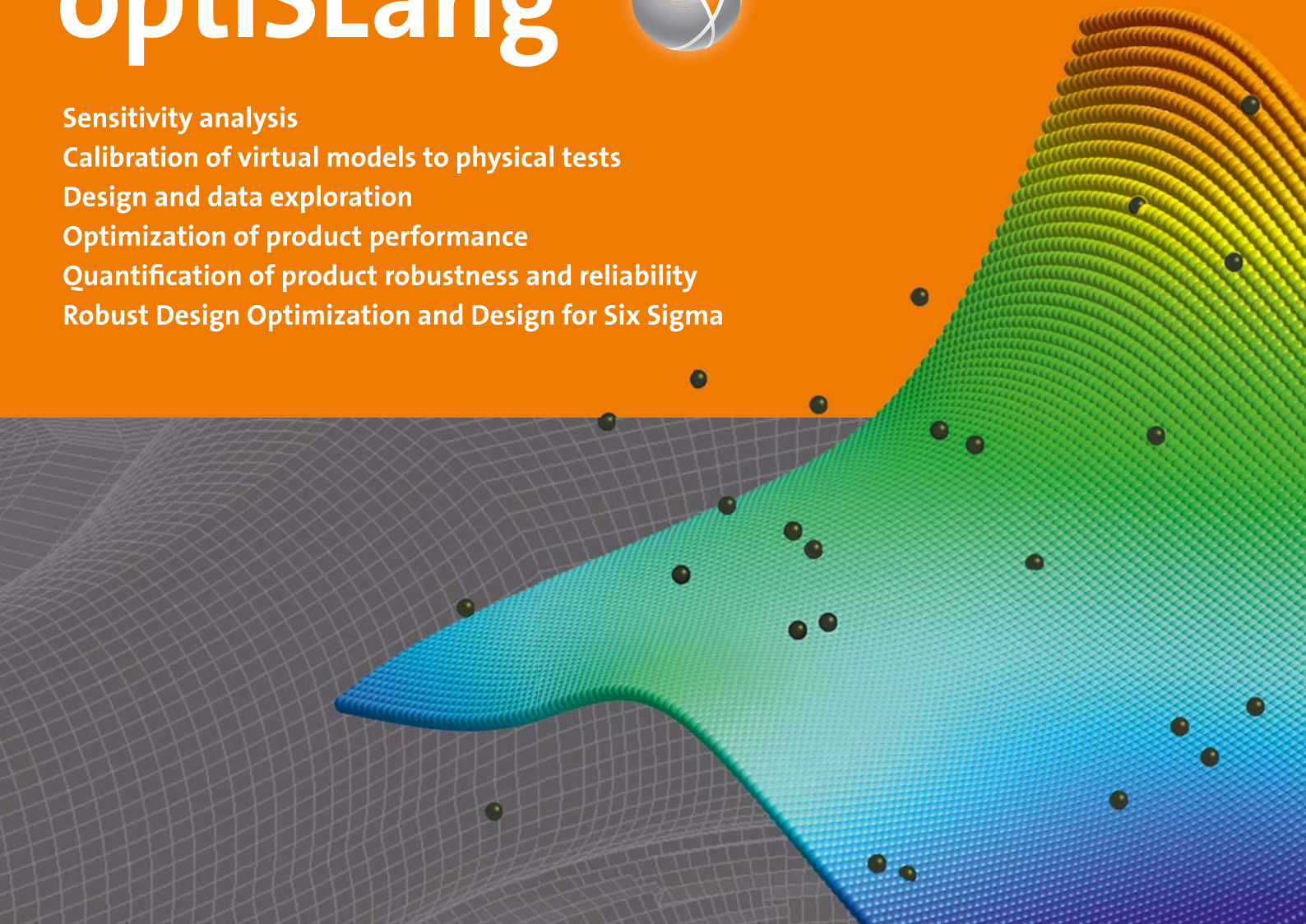
The case study was originally presented at the CASCON 2017 under the title “Automated optimization workflow with optiSLang for Rocky DEM simulations”.

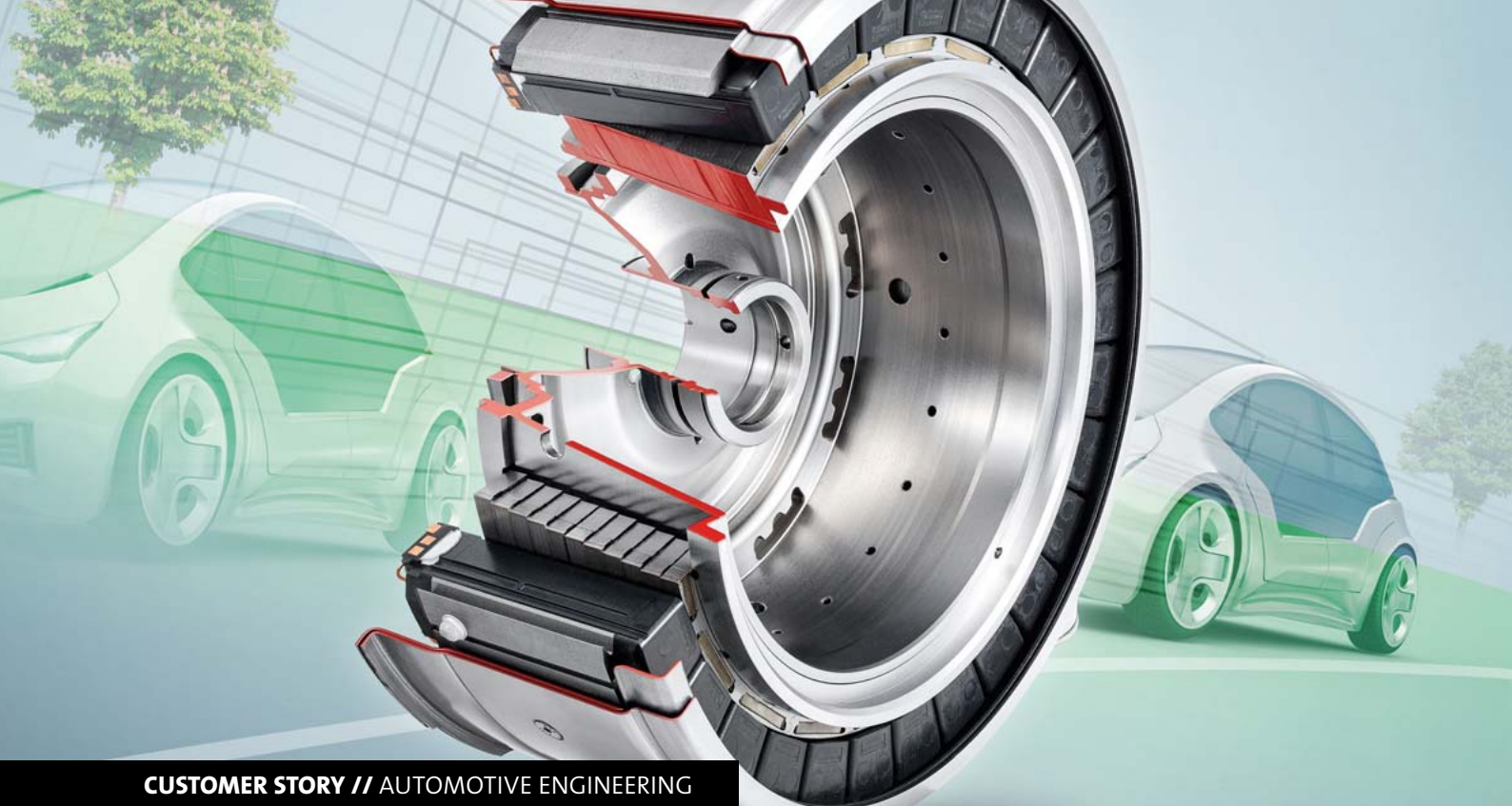
CAE Software & Consulting

optiSLang[®]



Sensitivity analysis
Calibration of virtual models to physical tests
Design and data exploration
Optimization of product performance
Quantification of product robustness and reliability
Robust Design Optimization and Design for Six Sigma





CUSTOMER STORY // AUTOMOTIVE ENGINEERING

ENGINEERING E-MOTORS

Creating an optimal custom engine for hybrid and electric vehicles requires that multiple electronic and mechanical components are designed and tested together as a system. Identifying and choosing trade-offs is difficult, but EM-motive GmbH tackled this challenge by developing a multidomain workflow incorporating ANSYS simulation and ANSYS optiSLang optimization software.

When car manufacturer Daimler formed a joint company in 2011 with Bosch, the world's leading automotive supplier, the synergy between the two companies was obvious. The joint company, EM-motive GmbH, combines Daimler's expertise in fuel cells and batteries with Bosch's knowledge of the development and production of electric motors to design and manufacture electric traction motors for electric and hybrid vehicles. Because the motors are designed to be modular, they can be adapted to fit a variety of vehicle classes and meet specifications for many different vehicles. Since 2012, the company has manufactured more than 300,000 e-motors for client companies throughout Europe. Even with this combined expertise, manufacturing a modular engine is complex and challenging. In addition to the main engineering constraints (cost, mounting space for the motor, cooling and inverter-specific properties), the customer-based requirements for each type of engine cover a wide breadth of individual physical domains:

- Thermodynamics: coolant flow rate and temperature, environmental temperatures, as well as winding and magnetic temperatures
- Structural mechanics: mounting space, torque, power, speed, tolerances to other parts and forces on bearings

- Electrical engineering: voltage, current, inverter-specific properties
- Efficiency and acoustics: airborne and structure-borne noise

To make the challenge even greater, all of the parameters to be optimized have to be considered simultaneously. Other factors must also be taken into account: noise, vibration and harshness (NVH); safety; and the cost of the engine. The engineers at EM-motive realized that, in such an interactive environment, a "classic" component development system, where rigid specifications for each component are designed separately and then assembled, was no longer possible. Instead, the company developed a design workflow that incorporated simulation throughout to account for the dynamic interactions between the components, as well as all the necessary parameters to determine optimal solutions and ensure design robustness.

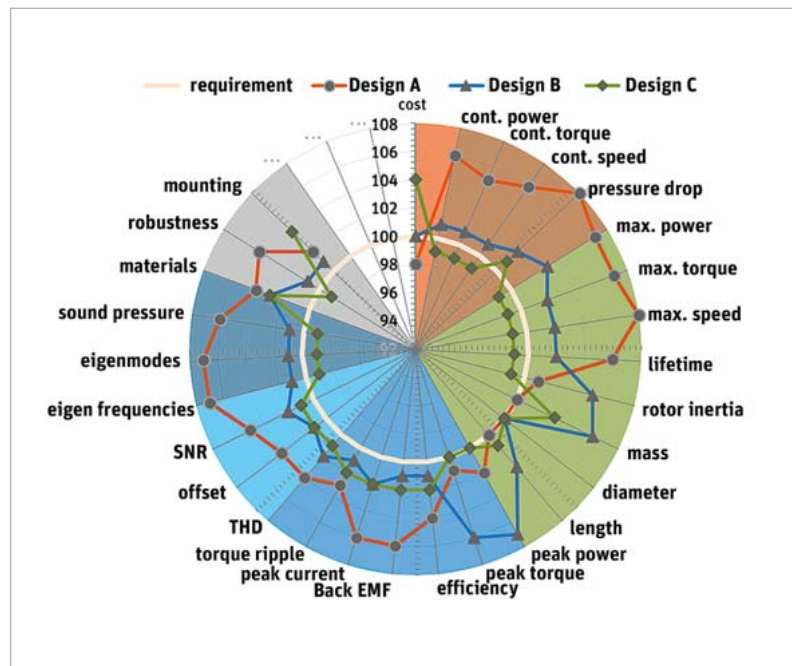
The parametric workflow to support sensitivity analysis, design optimization and design robustness evaluation includes ANSYS simulation software and other software tools, and was built and hosted in ANSYS optiSLang. These workflows help EM-motive to develop electric motors

within challenging time and cost requirements, as well as resolve customized design challenges, such as a late-stage customer requirement change for an engine design. As an example, a customer requested that the maximum speed for a particular engine needed to be increased by 1,000 revolutions per minute (rpm). The centrifugal forces of the accelerated speed, however, would cause the rotor design to fail. The engineers could increase the bridge thickness of the pockets for the magnets that are punched into the rotor lamination to withstand stress caused by the higher centrifugal forces.

However, this would increase the flux leakage in the rotor itself, causing reduced torque and power. An option to address this reduction is to increase the current in the windings (but only if higher current is available from the battery and electronics system). This solution would intensify losses and reduce efficiency, and was not acceptable to the customer. It was therefore necessary to redesign the entire engine to comply with all requirements. Fortunately, the EM-motive simulation workflow can be flexibly adapted to analyze the requirements for a specific engine, simulate all the dynamic interactions between the components, and present the customer with a solid understanding of the trade-offs for each design decision. The workflow provides the foundation to determine the best compromise for often contradictory goals.

A Workflow for Digital Exploration

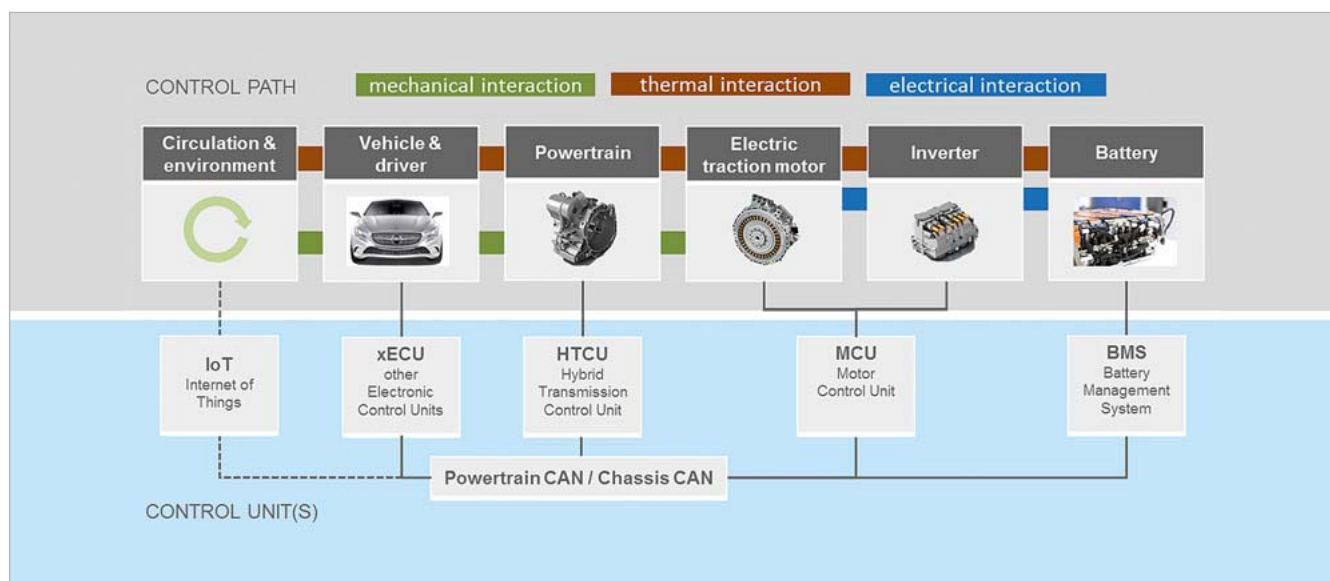
During the procurement phase, using ANSYS optiSlang workflow connected to CAD and employing specialized



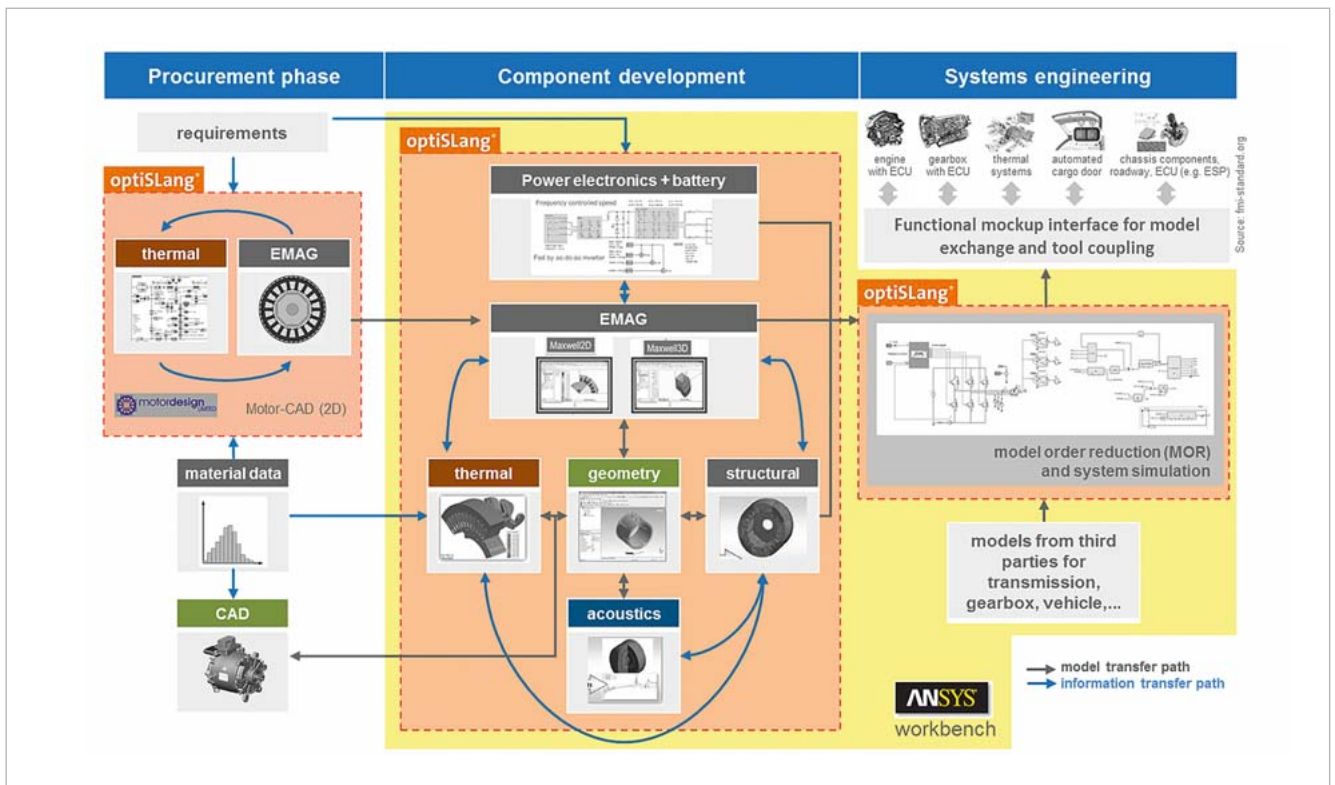
A radar chart illustrates three design concepts and how well they meet customer requirements.

electromagnetic-thermal software, the design engineers have the freedom to explore possible variations and their tolerances to fulfill customer requirements. They can then provide a fast answer so the customer will know if the requirements can be met with available motors or if new motor development is needed.

Through a set of iterative phases in which additional requirements are added, a new motor is designed and optimized using ANSYS simulation software in all the relevant physical domains. A shared interface with the ANSYS Simpler systems simulator helps them analyze the influence of power electronics on the motor. Because there is a bidirectional interface between ANSYS DesignModeler and the



The design workflow for an electric motor must comprise all of these internal and external components.



The three phases of the workflow are iterative as the designs are optimized

CAD system, engineers can create parameterized models of auxiliary geometries, such as the housing, and integrate them into the system design. The ANSYS tools allow the designers to use the results of one type of simulation as a boundary condition for another. They can then use forces from an electromagnetic simulation with ANSYS Maxwell as initial data for a structural mechanical simulation with ANSYS Mechanical. Using the various ANSYS tools integrated through ANSYS Workbench makes it possible to create a completely coupled simulation of the electromagnetic, mechanical, thermodynamic and acoustic domains.

With these parametric workflows in place, all important physical domain sensitivity studies within the relevant design space, as well as tolerance determination, can be conducted. The engineers can add further optimization loops, but because of the conflicting character of many discipline goals and constraints, and because of the need to quickly check the motor behavior on a systems-simulation level, reduced-order models (ROMs) must be extracted. Using the integrated equivalent circuit extraction (ECE) toolkit within ANSYS Maxwell or ANSYS optiSLang's data-based ROM generation, the team can extract reduced models for an overall system simulation.

Systems Modeling

These reduced-order models can be coupled in ANSYS Simploter to create a complete system simulation. Again a parametric workflow is built within optiSLang and, optionally, other third-party models can be integrated, such as a

transmission model or a complete vehicle model. At this point, the engineers might perform a system optimization loop to analyze the interactions between the components by varying parameters such as those for the controller.

Finally, to make the model interchangeable with additional engine components designed by outside parties, the designers use the industry-standard functional mock-up interface (FMI) to create models of the individual components, called functional mock-up units (FMUs). These FMUs are created with third-party software and can easily be exchanged while maintaining IP confidentiality: Since they contain only standardized inputs and outputs, the product-specific know-how is only accessible to the manufacturer. Another advantage of FMUs is that they can be imported into all current software packages for system simulation and can describe, for example, the behavior of the e-machine as a single component in the simulation landscape of a customer or development partner.

Understanding the Options

The final challenge is to present the optimized designs so that the customer can clearly understand the different design choices and their trade-offs. EM-motive developed a single radar diagram that transforms all performance indicators into dimensionless variables using the requirements as standardization values. It includes all domains and their requirements, further highlighted with a colored pie chart in the background, to clearly represent the domains. All points that are located outside of the 100 percent reference

circle meet the design requirements. Interactions between physical domains are also easily depicted in the diagram. If, for example, a design should be revised to improve acoustics, the mostly negative effects on efficiency are plainly shown. The chart provides a comprehensive understanding of the strengths and weakness of each redesign and how it fulfills (or doesn't fulfill) their unique requirements.

Engine design, like many complex processes today, requires a collaborative, systemic approach to be successful. EM-motive's systemic approach to engine design integrates the ANSYS parametric simulation environment and an innovative presentation method to ensure that their automotive manufacturing customers can develop the next generation of hybrid and electric vehicles within challenging time and cost constraints.

Author // Marc Brück

(Senior Expert Simulation Technology, EM-motive GmbH, Hildesheim, Germany)

This article was adapted from an interview by the editorial team of the CADFEM Journal.

Images by courtesy of EM-motive.

Getting Started

Sensitivity analysis, multiobjective and multidisciplinary optimization, robustness evaluation, reliability analysis, model calibration and Robust Design Optimization

optiSLang SoS



Info-Events

Webinar Series | In short introductory webinars, we will explain the added value of our software products in practical application examples from various areas of engineering.

Info Day | During an information day, you will get a comprehensive overview and you will have the opportunity to get in direct contact with our consultants in order to discuss specific tasks.

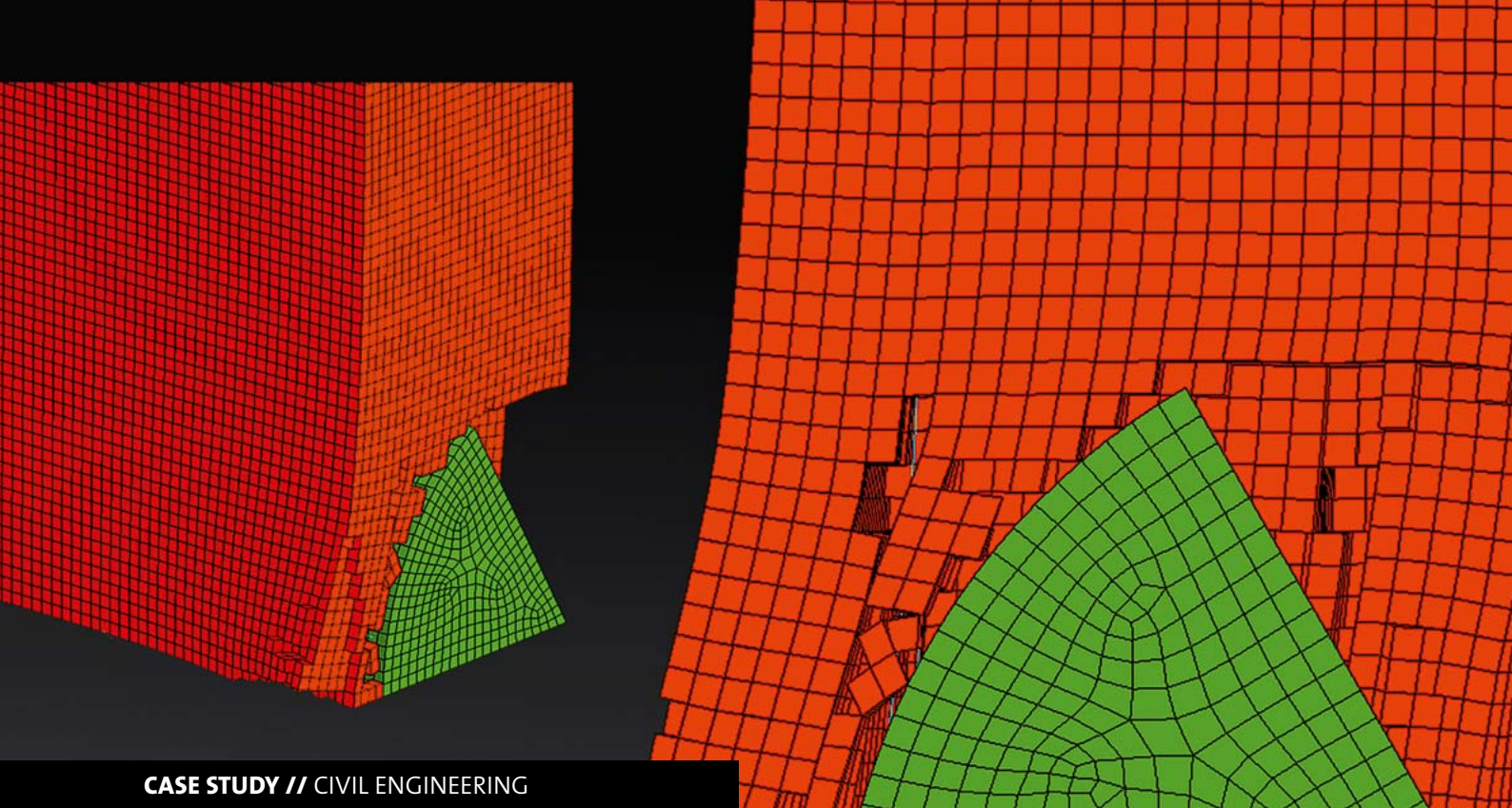
Introductory Training

During **one-day introductory courses** or various **E-learning units** we will acquaint you with the application of our software products by means of illustrative examples.

More ways for getting started are our offers for

Pilot Projects or Advanced Training

Please visit www.dynardo.de for detailed Information.



CASE STUDY // CIVIL ENGINEERING

SIMULATION OF BURST PROTECTION WITH ANSYS LS-DYNA AND OPTISLANG

Using ANSYS LS-DYNA and optiSLang, impact simulations were conducted for the proper design of burst protection walls made of reinforced concrete in turbomachinery test facilities.

Motivation and task definition

Rotating machines, e.g. turbines, generators and aircraft engines, are operated at high speed in real use as well as in rotary test facilities. In the event of a component failure (case of accident), persons and material in the immediate surrounding must be protected from the effects of flying debris by suitable burst protection devices [1]. For the burst protection of test facilities, either an immediate encapsulation of the rotating machine or the installation of separating walls, e.g. between test and measuring facility, can be considered.

In case of an accident, it is assumed that bursting fragments of the rotating machine will hit the protection walls at high speed. The wall thickness has to be dimensioned in a way that fragments cannot punch through or cause chipping on the off-load side.

This article presents a procedure for the design of burst protection walls made of reinforced concrete which are suitable for rotary test facilities. A sufficient dimensioning can be verified by means of non-linear, transient dynamic studies using ANSYS-LS-DYNA as well as by conducting a subsequent sensitivity analyses for different load scenarios with ANSYS-optiSLang.

Simulation solutions

Assumptions for the description of the load scenario

Impact loads on burst protection devices are considered to be accidental design situations according to DIN EN 1991 [2]. The load specifications (e.g. breakage and flying debris of turbine blades or fragments of rotating disks) must be defined according to available standard assumptions (e.g. [1], protection category D), engineering assumptions as well as experience of the plant operator. Sensitivity analyses, carried out with ANSYS optiSLang, revealed the influence and the effects of individual load assumptions on the burst protection device.

In this case, a third slice load fragment was chosen (see Fig. 1) as a basis for the impact definition. The full rotational energy of the third slice is supposed to be converted into translational energy, from which a corresponding translational initial speed for the impact of the fragments on the wall is derived. The largest rotational energy of the different experimental devices defines the worst case scenario. The stiffness of the fragment is assumed with the Young's Modulus of steel (210000 MPa). A plastic energy dissipation of the fragment is not considered.

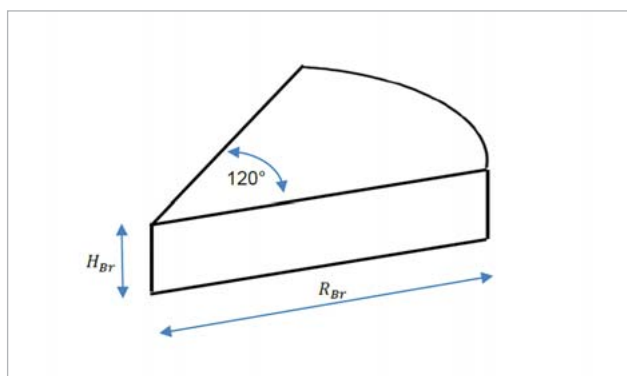


Fig. 1: Geometry of fragments (schematic illustration)

Non-linear resistance of reinforced concrete under impact load

The description of the non-linear resistance of reinforced concrete is based on the normative specifications in DIN EN 1992 [3] with consideration of [4] for non-linear methods (see section 5.7). The material properties of the concrete and reinforcing steel according to [3] are used for the respective concrete or reinforcing steel class, as well as the partial safety factor for resistance $\gamma_R = 1,1$ required for accidental design situations.

However, the normative specifications still need to be extended for this transient dynamic impact analysis. Regarding concrete and reinforcing steel, a strain rate-dependent increase in strength can be particularly observed

under impact load. Among other things, this effect was analyzed for concrete in [5]. In order to take this effect into account in the FE analyses, the strain rate-dependent increase of concrete compressive strength is considered according to the CEB recommendation for concrete with a compressive strength of 50 MPa, specified in [5]. The correlation can be seen in Fig. 2.

For concrete, the elasto-plastic LS-DYNA material model * MAT_PSEUDO_TENSOR with Mode II.C. ("Tensile failure plus damage scaling") [6] is applied. Therein, the shear failure of the concrete is described by an elliptical flow condition and the softening by means of a damaging function.

The non-linear material behavior of the steel is represented by the LS-DYNA material model * MAT_PIECEWISE_LINEAR_PLASTICITY [6]. The strain rate dependence is derived according to [7] with a strengthening coefficient of about 1.15 at a strain rate of 10 s^{-1} . A multilinear stress-strain curve is defined, taking into account a softening caused by the effect of reinforcing steel necking. If a failure strain of 6% is reached, the elements become deleted from the system (eroding).

Finite Element simulation model

The burst protection walls made of composite reinforced concrete are represented by a discrete, spatial modeling of concrete and reinforcing steel. Steel bars were chosen for the reinforcement of the burst protection walls. The concrete is discretized by volume elements, the individual rein-

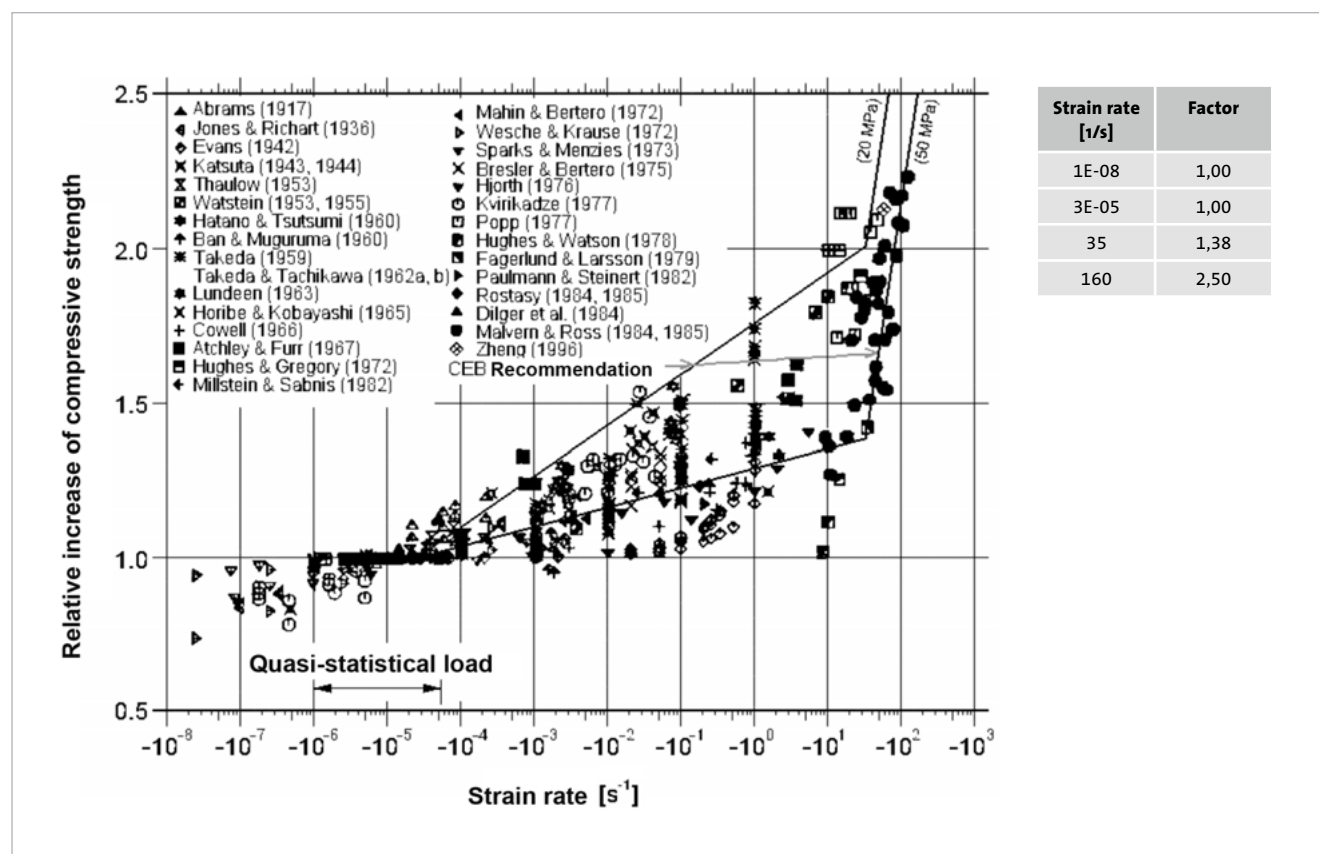


Fig. 2: Dependence of concrete compressive strength on the strain rate according to [5] (Fig. 2.18)

forcing bars by means of beam elements. A complete bond between reinforcing steel and concrete is assumed and implemented in the FE model by the use of equal nodes of the concrete's solid elements and the beam elements of the reinforcing steel.

The finite element model (FE model) is shown in Fig. 3. For the design of the burst protection walls, the FE model is parametrically created, thus the wall thickness, the reinforcement ratio, the type of concrete, the place of impact, as well as the load parameters of the fragment can be varied.

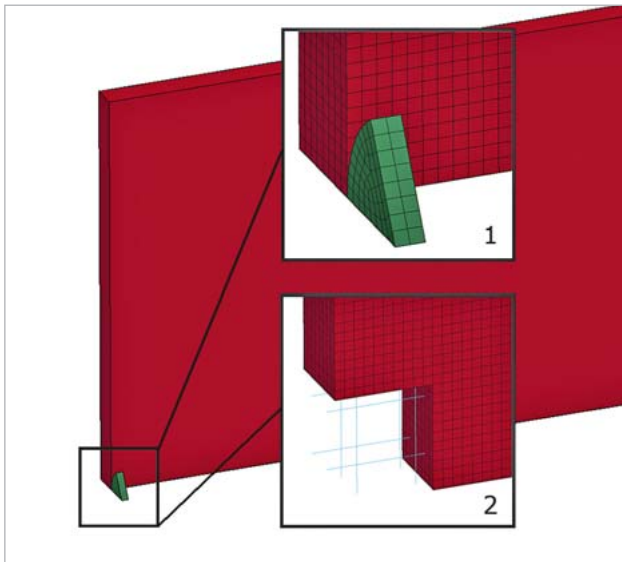


Fig. 3: Double-symmetrical FE model of the burst protection wall; 1-fragment, 2-reinforcement

Definition of boundary conditions

The horizontal load transfer of the burst protection walls is via the floor and transverse walls, as well as over the cover plate (at test stand 1) or the ceiling (at test stand 2). In the FE model, the effects regarding the cover plates on the booths in test stand 1 are idealized by two limit states (two analyses). In the first analysis, the burst protection wall is assumed to be supported by the cover plate perpendicular to the surface of the wall. Thus, a four-sided supported wall is applied in the finite element model. The impact position of the fragment is defined vertically and horizontally in the center of the burst protection wall, as this is assumed to be the worst-case impact position for a four-sided supported wall.

In the second analysis, the supporting effect of the cover plate is unconsidered, which is represented by a three-sided supported wall in the FE model. Here, the impact position of the fragment is located vertically on the upper edge (unsupported edge) and horizontally in the center of the burst protection wall, which is assumed to be the worst-case impact positions for a three-sided supported wall.

Those booths of the test stand 2 which are all covered with a ceiling are represented by a four-sided supported wall in the FE model. The impact position of the fragment is applied analogously to the first analysis at test stand 1

vertically and horizontally in the middle of the burst protection wall. Corresponding symmetry conditions are used depending on the applied double-symmetrical or half model.

The load on the burst protection walls results from the mass m_{Br} and the initial speed $V_{0,Br}$ of the fragments. The initial speed is derived from a translational energy, which is fully generated by the rotational energy of the fragment.

Simulation of design variations

During a first variant study, both the wall thicknesses from 150 mm to 500 mm as well as the reinforcement ratio are incrementally increased in order to determine the smallest thickness that is still capable of preventing fragments from punching through the wall. In addition, constructive boundary conditions (e.g. bar diameter, bar spacing, concrete cover) are considered in these analyses.

The analyses reveals that the impact position of the fragment has no relevant influence on the results. This can be explained by the conservation of momentum and the much higher mass of the burst protection wall compared to the fragment.

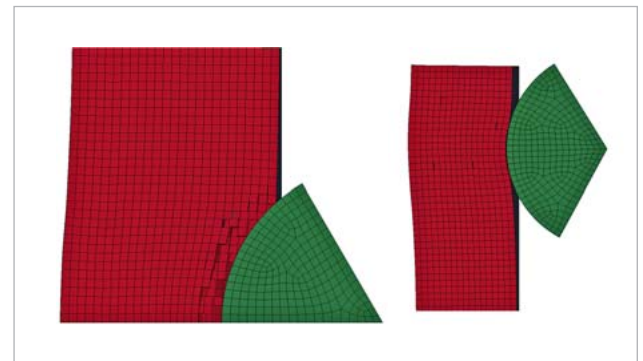


Fig. 4 Sample plots for the state of final deformation regarding an impact area located in the middle and at the upper edge

Sensitivity analysis

As a part of the sensitivity analysis, four parameters are varied which describe the shape as well as the kinetic energy of the fragment:

- the speed of the rotor, i.e., the translatory speed
- the radius of the fragment
- the height of the fragment
- the mass of the fragment

The sample selection was carried out with ANSYS-optiSLang by using Latin Hypercube sampling. This method generates uncorrelated, uniformly distributed input variables covering the specified variation ranges.

The aim of the sensitivity analyses of both test stands is to identify the initial kinetic energies of the fragments when the burst protection walls of the test cells are about to break or chipping starts on the off-load side. For this purpose, response values of the penetration depth of the fragment and

of the maximum kinetic energy are determined. In addition, a visual examination of the damage is done by evaluating the plots from the off-load side of the wall. The wall is considered to be inadmissibly stressed if it shows damage on the back side (stripped, accelerated fragments).

Some results are exemplarily shown in Fig. 5 and Fig. 6. The variation of the maximum penetration depth (parameter maxU) is influenced by the variation of the three input parameters mass, height and speed. As shown in Fig. 5 top, mass has the greatest influence with 53.5%, followed by speed with 33.1% and height with 19.8%. However, the variation of the radius has no relevant influence on the variation of the penetration depth. The results also indicate that the loading on the wall does not depend on the stiffness of the fragment but on its impact area. Fig. 5 bottom shows the Metamodel of Optimal Prognosis (MOP) for the maximum penetration depth as a result of the sensitivity analysis. The penetration depth (maxU) tends to decrease if the impact area (height of the fragment) rises. The influence of the height for smaller fragments is nearly linear. For a fragment mass approximately higher than 3 kg, the influence of the height shows exponential characteristics.

Fig. 6 shows the determined correlation between penetration depth and kinetic energy. Using these results, the plant operator is also capable of verifying future samples and load scenarios with regard to their impact on the demands of burst protection.

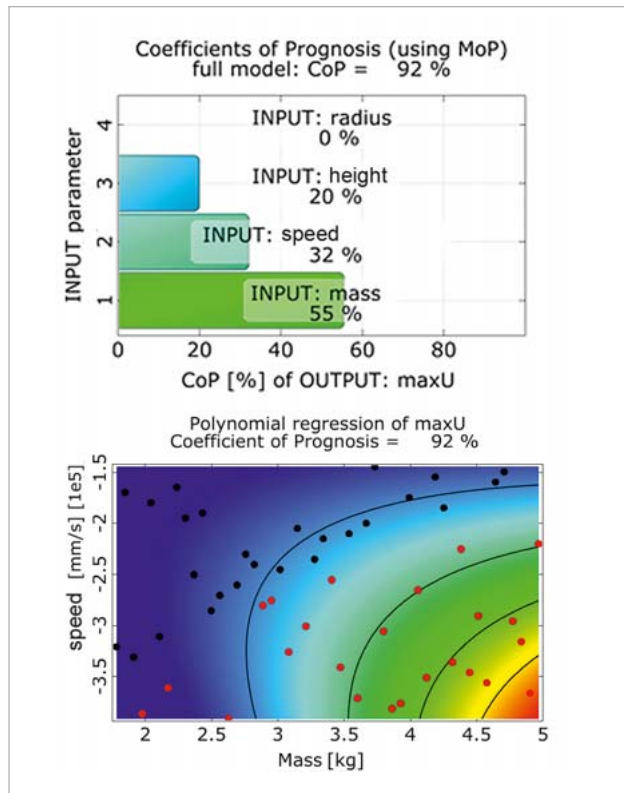


Fig. 5 top: Prognosis measures CoP of the penetration depth (maxU) compared to the input parameters; bottom: Metamodel of Optimal Prognosis (MOP) to visualize the dependence of the fragment's penetration depth regarding the load parameters v and m

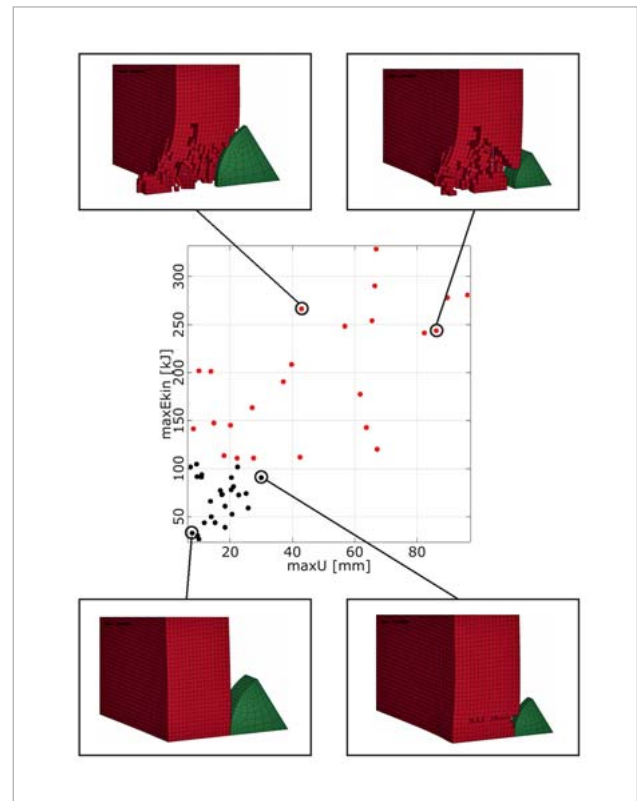


Fig. 6: Pairwise dependence of the kinetic energy regarding the penetration depth

Summary and conclusions

The presented simulation procedure supports the safe design of reinforced concrete burst protection walls according to the requirements of the operator.

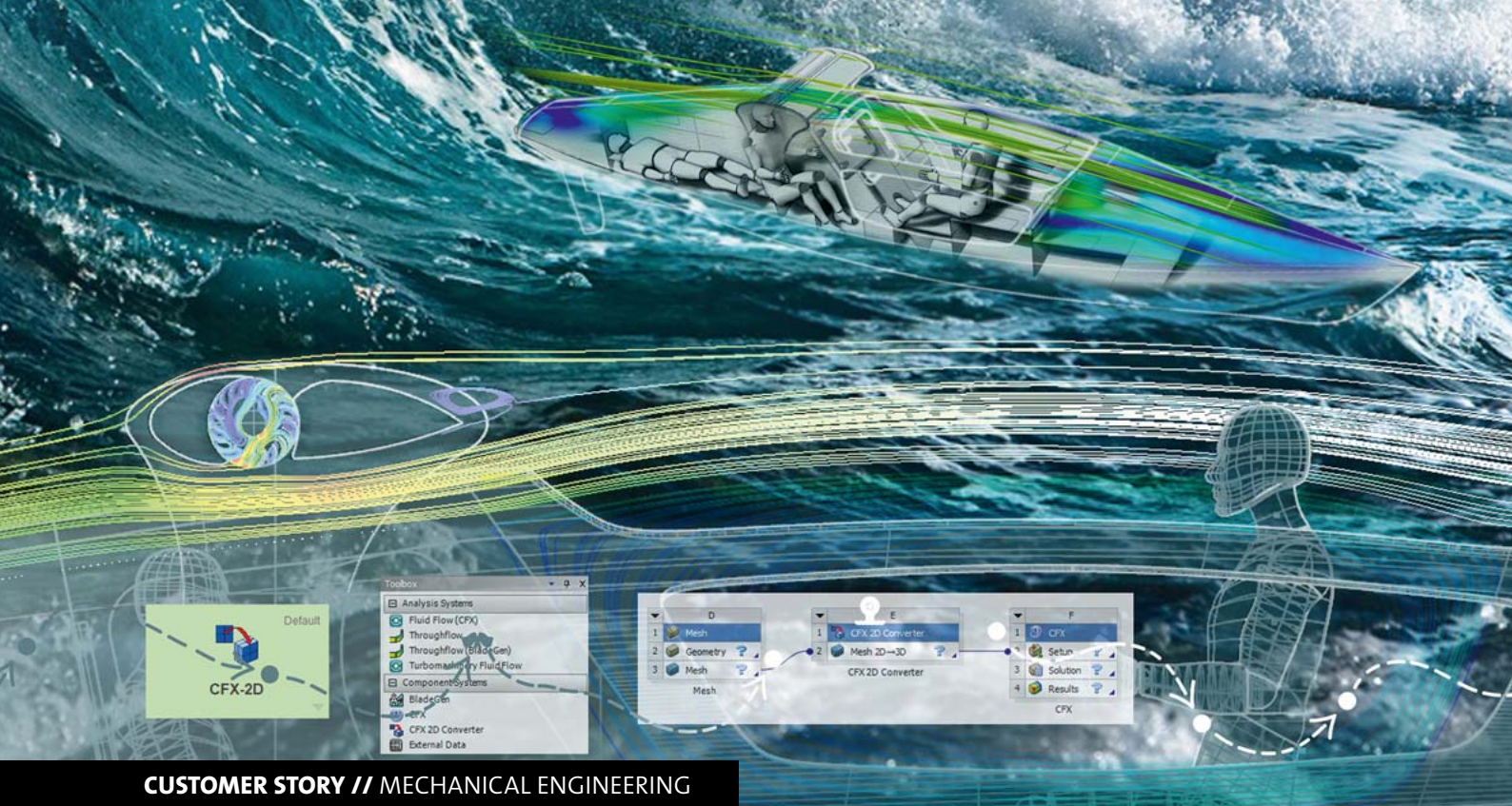
Considering the ultimate limit state analysis (DIN EN 1992-1-1: 2011-01, Eurocode 2), a safety related to the actions on the structure could be determined. Besides a conservative description of the affecting loads, it is of crucial importance for such tasks to conduct a realistic simulation of the nonlinear material and crack behavior of the reinforced concrete. Here, a sensitivity study indicates the scattering ranges of load parameters with a sufficient burst protection. These results support operators of test facilities to quickly estimate permissible load scenarios for future tests.

Authors //

R. Schlegel, T. Dannenberg, T. Seider (Dynardo GmbH)

Source //

www.dynardo.de/bibliothek/industriefelder/bauwesen/Berstschtzberechnungen_mit_ANSYS-LSDYNA



CUSTOMER STORY // MECHANICAL ENGINEERING

DESIGN OPTIMIZATION OF A WIND TURBINE FOR THE ROWING BOAT “AKROS”

The ANSYS optiSlang optimization toolbox was used together with ANSYS CFX fluid dynamics software package in order to find an optimal wing and rotor geometry.

Motivation

At the end of 2018, the famous Russian adventurer Fedor Konyukhov is going to set his solo round-the-world sailing on the rowing boat AKROS from Australia to Cape Horn. The journey will start from the Australian island of Tasmania. Konyukhov will sail south of New Zealand to the Pacific Ocean to meet the largest stretch of the Southern Ocean. The entire route is 9,000 km.

Sailors call the areas between the latitudes of 40 and 60 degrees south the “Roaring Forties”. The average wind speed in these latitudes is 10-15 m/s (6-7 on the Beaufort scale), reaching 30-40 m/s during violent storms which are regular in this area. Icebergs can be seen all year round across the Southern Ocean. Some of them may reach several hundred meters in height.

The new AKROS boat was designed on the basis of the TURGOYAK rowing boat sailed by Konyukhov in 2016, during his world-first circumnavigation. The design has to be adjusted to extreme sailing conditions. To build a new rowing boat, British designer Phil Morrison was invited. He designed the two boats for Konyukhov: URALAZ and TURGOYAK. The size of the new boat will be 9 meters. The forebody will be divided into two watertight compartments

with an additional “crash box”. The structural design of the boat is shown in Fig. 1.

The preliminary design shows that crossing the ocean at low temperatures will require an additional source of electric power to heat the stern compartment with a navigation room, a cook galley and a recreation compartment. The main source of electric power of the TURGOYAK is solar panels. SimuLabs engineers suggested that the additional source of power for the AKROS boat should be a small wind turbine. The engineers developed and patented a revolutionary configuration and design of the wind turbine which deals with the ship’s stability and slightly increases the specific resistance of the boat.

Rowing-boat wind turbine

The main component of the wind turbine is a wing airfoil containing a contoured duct connecting the opposite wing surfaces. The induced air drives the turbine and the associated generator. The basic design of the wing ensures that all of its components are fixed to increase the reliability of the wind turbine. To find the optimal wing and rotor geom-

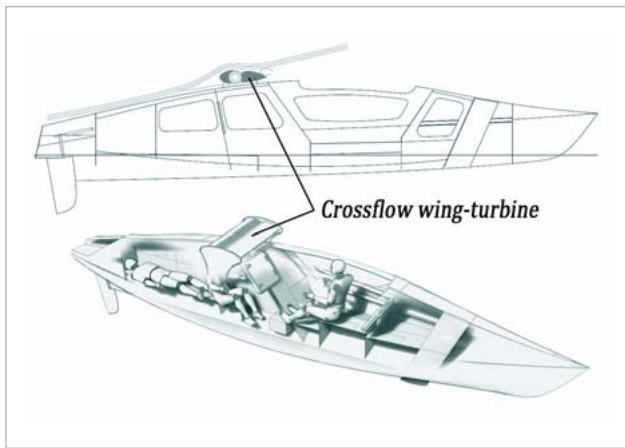


Fig. 1: Structural design of the AKROS rowing boat

etry, the ANSYS optiSlang optimization toolbox was used together with the ANSYS CFX fluid dynamics software package. The designed turbine capacity at a wind speed of 15 m/s and a specific speed of 0.3 is 100 W. The weight of the turbine including the generator is not more than 10 kg. A similar horizontal-axis wind turbine due to dimensional constraints produces no more than 35-40 W at a higher specific speed.

Simulation and mathematical models

Optimization was based on varying the geometries of the rotor blades, the composite wing, and the gap between the rotor and the contoured duct inside the wing.

Due to the fact that optimization is resource-intensive, the priority was selecting the right approach to the blading nomenclature to define the blade profile shape with the minimum number of optimization variables. This significantly speeded up the optimization.

Geometry parameterization of the turbine rotor blade with six dimensional parameters is shown in Fig. 2. The geometry of the blade profile was updated by modifying the leading blade angle *LeadingAngle*, the blade chord *Length*,

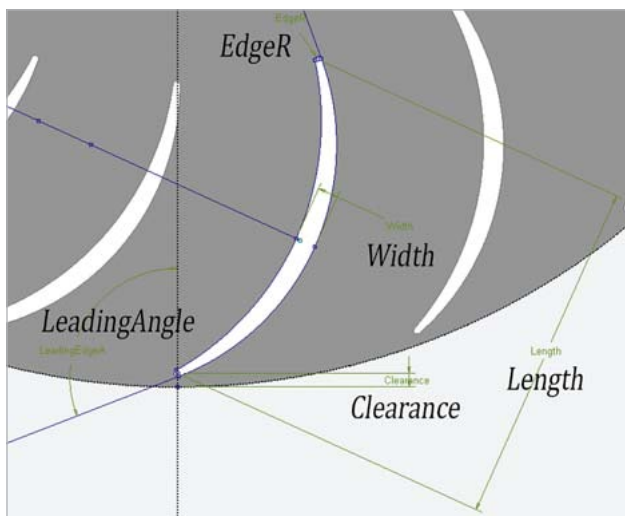


Fig. 2: Simulation model of a wind turbine

the maximum profile width *Width*, the leading edge radius and the trailing edge radius *EdgeR*. The two additional dimensional parameters were used for the number of blades count and the gap between the rotating rotor as well as the fixed duct inside the wing *Clearance*.

The aim of rotor geometry optimization was to maximize the wind turbine efficiency and power with regard to the rotor speed constraint and geometries of the turbine.

In all simulations, the airspeed was assumed equal to 15 m/s, which corresponds to the average annual wind speed in the “forties”. The turbulence level was 5%. The curvature-corrected SST $k-\omega$ turbulence model was used.

Most of the simulations were carried out by a 2D frozen-rotor approximation. When using the Frozen Rotor approach, all steady-state simulations were performed simultaneously for all blade channels without a circumferential averaging. The obtained quasi-unsteady flow field determined the interaction between the rotor and the stator quite accurately and did not require many computational resources, which was critical to optimization.

At the design completion stage, a number of 2D and 3D steady-state simulations were performed for the optimized turbine geometry.

In order to obtain convergence to a two-dimensional steady-state solution in ANSYS CFX 18.2 with a residual of $10e-5$, nearly 130 iterations were required.

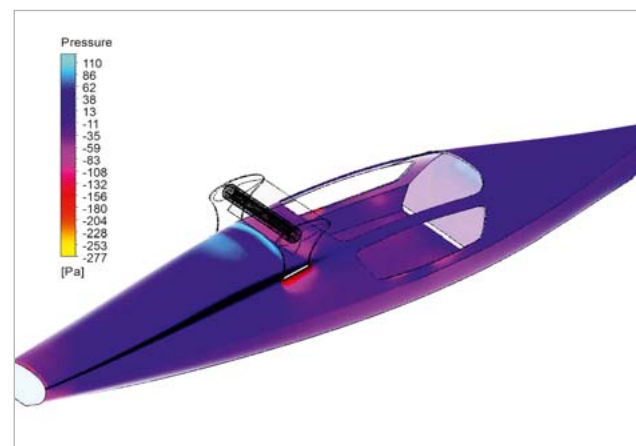


Fig. 3: Unsteady-flow simulation of a wind-turbine boat hull

Geometry optimization process

Geometry optimization of the rotor was performed with the ANSYS optiSlang toolbox and involved the following steps:

1. Sensitivity analysis
2. Parametric response surface modeling
3. Response surface optimization
4. Validation of the Pareto optimal solutions

According to the sensitivity analysis, there is no linear relationship between the pairs of input parameters (no correlations close to 1 or -1). The correlation values mostly



Fig. 4: Parameter correlation matrix

Parameter	Minimum value	Nominal value	Maximum value
Length	30 mm	50 mm	60 mm
EdgeR	0.25 mm	0.5 mm	1 mm
Clearance	0.5 mm	1.5 mm	2 mm
LeadingAngle	100°	110°	130°
Width	1 mm	3 mm	6 mm
Count	15	17	19
TSR	0.3	0.3	0.65

Table 1: Response range of dimensional parameters

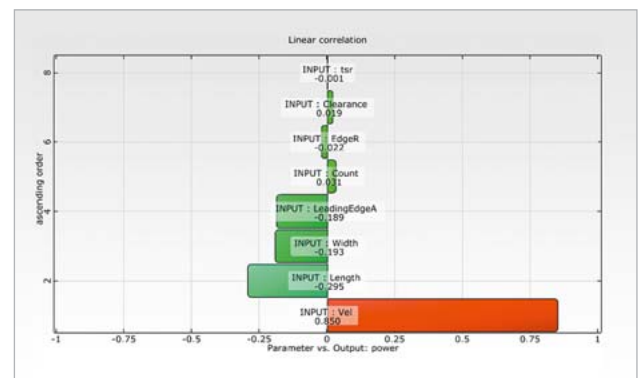


Fig. 5.: Effect of parameters on the wind turbine power

range between -0.5 ... + 0.5 making it clear that there is either no mathematical correlation between the parameters or the correlation is highly nonlinear. There is a nominal non-zero correlation between quite obvious pairs of parameters, for example, the turbine power and the airspeed.

Correlation calculation and response surface modeling required 155 solver calls, i.e., 155 design simulations of the turbine rotor. From the set of simulation points, a response surface was modeled (surrogate/substructure response models) and a Coefficient of Prognosis was estimated.

A Coefficient of Prognosis (CoP) of 95% indicates that the response surface matches well with the design response and may result in successful optimization.

The geometry optimization of the rotor was based on response surface methodology and required no solver calls. Alternatively, the so-called Metamodel of Optimal Prognosis (MOP) solver was used. This metamodel solver estimates the values of output parameters based on the values of input parameters.

The objective was to maximize the turbine power. The two geometric constraints for the selected parameters are critical keys for an accurate geometry and mesh modeling.

During the response-surface optimization, 7,900 points were counted with the MOP Solver and, subsequently, the Pareto front was found.

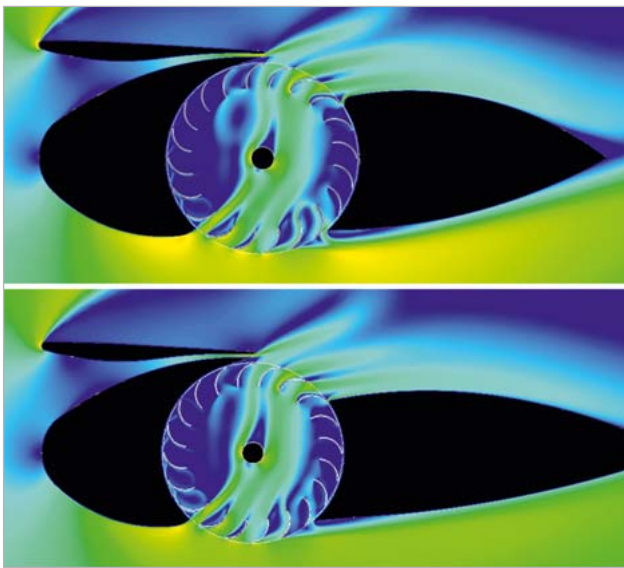


Fig. 6: 2D simulation of various turbine rotor and wing geometries

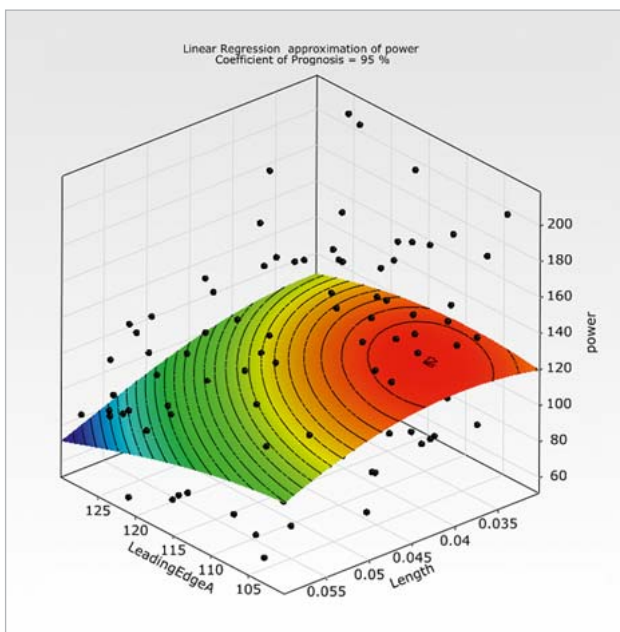


Fig. 7: Response surface

After the response-surface optimization, the optimal solution was validated, i.e., by using a full-scale design solver for the simulation of the design with optimal values of the input parameters.

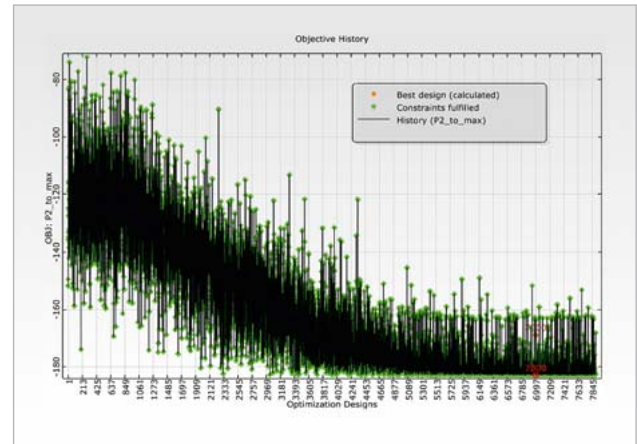


Fig. 8.: Optimization process convergence

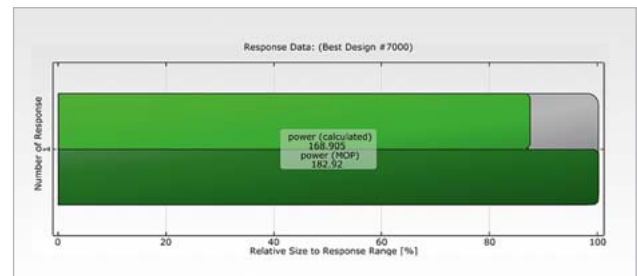


Fig. 9.: Power values: response surface vs. validated solution

Author //

Denis Khitrykh, Taras Shevchenko (CADFEM CIS, R&D Center 'SimuLabs')



CUSTOMER STORY // AUTOMOTIVE ENGINEERING

STATISTICAL APPROACH TO PREDICT SEALING PERFORMANCE

MANN+HUMMEL benefits from the use of optiSlang and its capability to develop increasingly cost competitive designs as an example for simulation driven product development.

Introduction

MANN+HUMMEL is a global leader and pioneers in filtration with a rich heritage and experience of more than 75 years in the business. Each second, 26 filters are produced, shipped, sold and installed worldwide. As a global player, MANN+HUMMEL understands the requirements and demands of the market, having its core business areas in automotive domain, industrial sector, intelligent air solution and water solutions.

Air filters in automobiles are an essential and integral component that prevents particles from entering the engine cylinder. When air filters are viewed as a system, there is the dirt side which is exposed to all the elements of the atmosphere, and then there is the clean side with filtered air, which later makes its way into the engine. In between these two stages, an effective form of sealing has to be present that prevents leakage of uncleaned air into the clean side of the filter. Thus sealing plays a crucial role in filtration and in turn engine life. Sealing is usually made of PU foams or elastomers, which are highly expensive. Hence the ultimate objective is to reduce the gasket volume by use of parametric modeling and by retaining adequate contact pressure with minimal mounting force that defines the sealing efficiency.

Methodology Approach

Focus of the article is to highlight the approach followed in the product life cycle. Hence for the purpose of representation, the air filter housing along with seal is simplified (Fig. 1). Sealing is considered as a gasket model where stiffness contribution in transverse direction is much smaller than the stiffness along the thickness. Clamps and hinges on the peripheral region compresses the gasket and provides adequate pressure to restrain leakage. Although the optimization of the housing and sealing profile can be combined together (Fig. 2) for a better discerning, both are addressed separately.

Seal profile optimization

Parametric Model

Seal profile optimization is carried out using 2-D sectional analysis. A parametric model of the seal is created within the given design space and constraints (Fig. 3). Parameters and their ranges are set based on the past product experience and manufacturing feasibility.

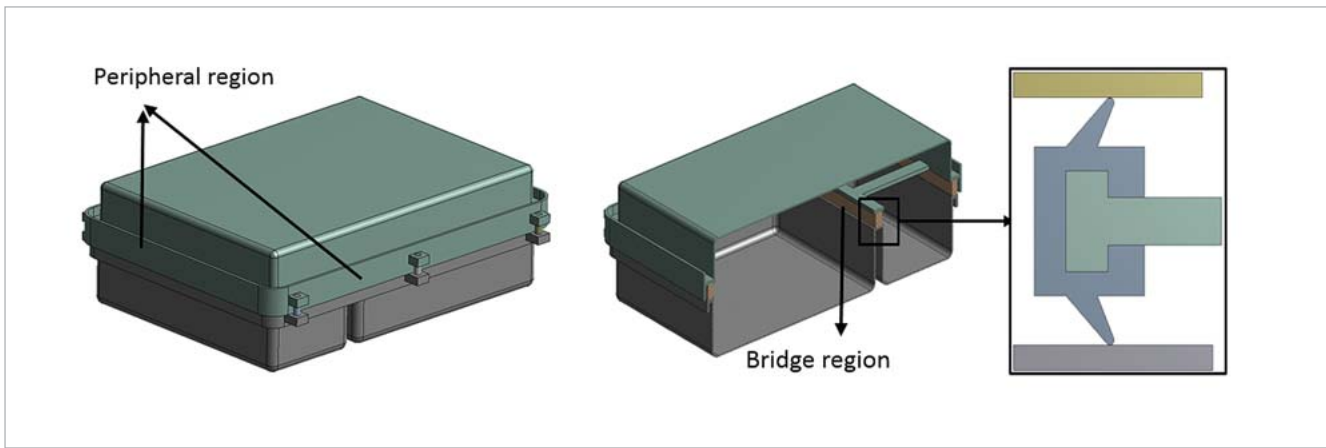


Fig. 1: Simplified Model of Air Filter with seal profile (reference model)

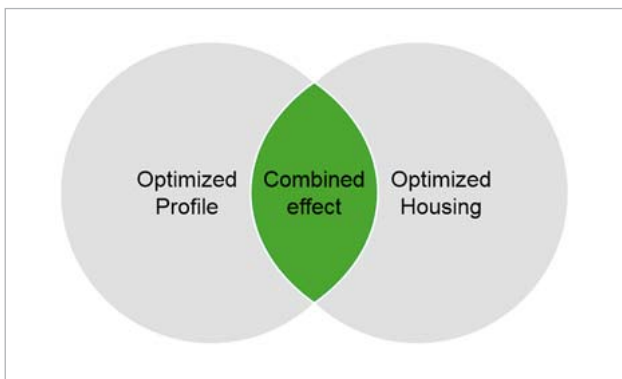


Fig. 2: Schematic representation of the approach

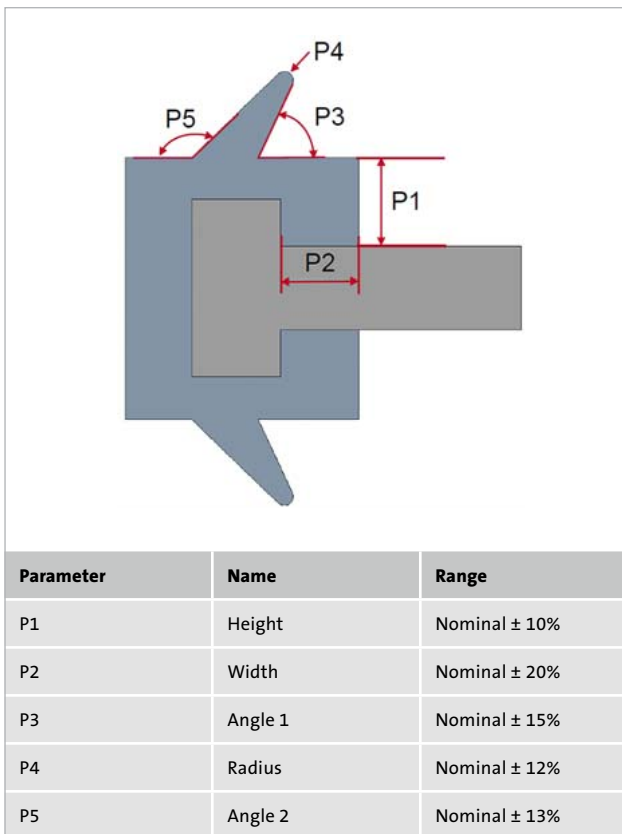


Fig. 3: Parameters and their range for seal profile optimization (reference model)

Boundary Conditions

Air filters are mounted in close vicinity of engines and are exposed to elevated temperatures. Roping in this fact, the analysis is carried out at high temperature. Gasket is assigned with ShoreA hardness and the frame inside the gasket with plastic respectively. Casing is fixed and seal is compressed with the cover to replicate the assembled condition (Fig. 4). Contact pressure, mounting force and volume are the important output parameters which are contemplated in order to achieve the optimized design.

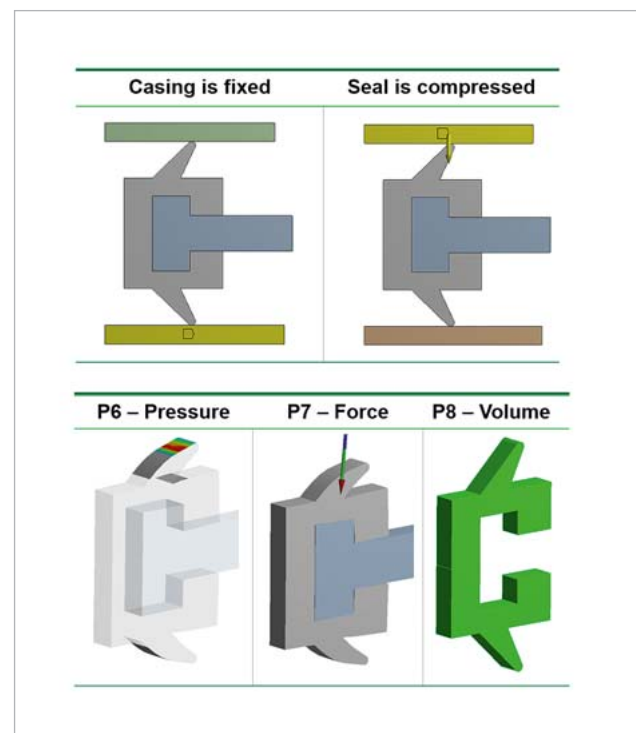


Fig. 4: Boundary conditions and output parameter (reference model)

Sensitivity Analysis

Sensitivity analysis is carried out to determine the major influencing parameters on the required output parameter. A large number of well laid out design points are employed to

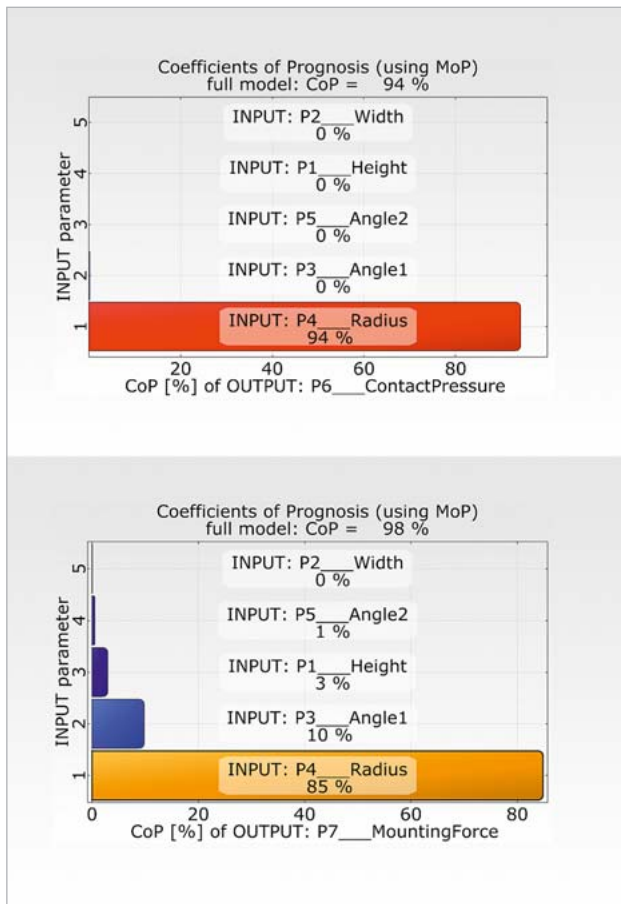


Fig. 5: CoP for contact pressure and mounting force

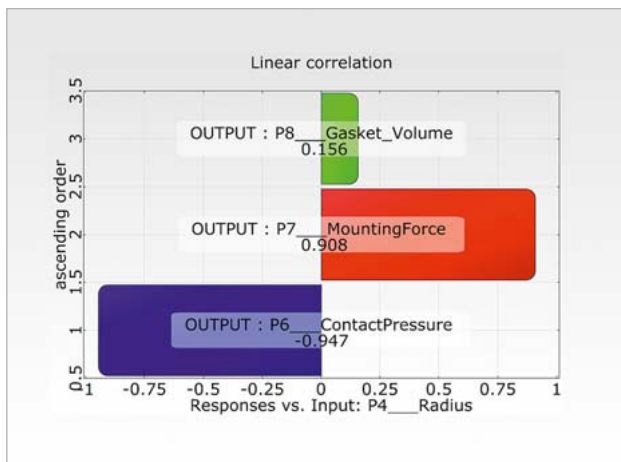


Fig. 6: Linear correlation for radius

capture the domain precisely using advanced Latin Hypercube Sampling method. Coefficient of Prognosis (CoP) for contact pressure and mounting force remains stable with radius being the major influencing parameter (Fig. 5). The parameter “P3 - Angle1” also contributes to mounting force to a certain extent. The linear correlation plot (Fig. 6) indicates that the increase in radius, decreases the contact pressure, increases the mounting force and gasket volume. With a robust CoP value as the primary quality measure, the outcome of sensitivity analysis is taken further into optimization.

Optimization

Optimization is performed to single out the best possible design within the given design constraints. Evolutionary algorithm is used for the same, as it provides added advantage of multiple constraints and objectives. Optimal contact pressure is necessary to prevent gasket leakage with the lowest mounting force for the safety of adjacent component during assembly. Minimizing the gasket volume to save on material cost, is an additional objective for optimization. Evolutionary algorithm estimates all possible input parameters to achieve exceedingly superior results (Fig. 7):

- Optimal contact pressure
- Reduced mounting force
- Minimized gasket volume

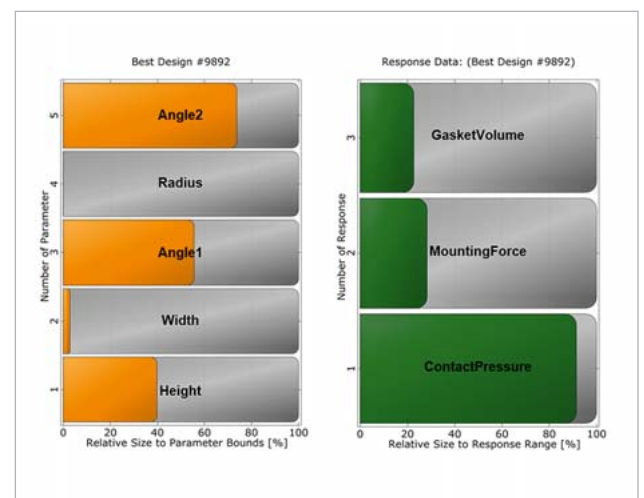


Fig. 7: Objectives, best input parameter and best output parameter

Cross Validation

With the best design parameters, a CAD model is constructed. Simulation is run with the same boundary conditions and material properties to cross validate the output from optimization. Difference between statistics and simulation (Fig. 8) was found to be within acceptable limits suggesting precise correlation.

Output	Difference	Checklist
Contact pressure	3%	<input checked="" type="checkbox"/>
Mounting force	1.2%	<input checked="" type="checkbox"/>
Gasket volume	0,8%	<input checked="" type="checkbox"/>

Fig. 8: Difference between statistics and simulation

Results

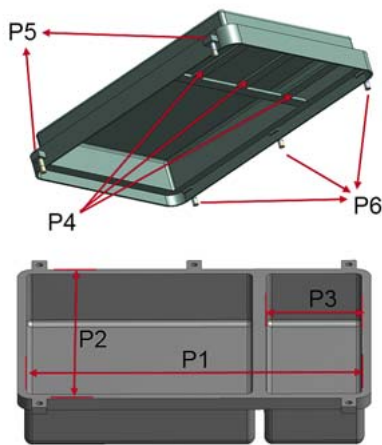
Comparing nominal design with that of the optimized, the contact pressure and mounting force was the same but the

gasket volume was reduced significantly by 13 %. In such cases, a balance has to be struck by drawing a line whether to have a certain sealing efficiency with corresponding gasket volume.

Housing optimization

Parametric Model

Parametric model of the housing is constructed based on the design space provided by customer. The entire parametric model is built from scratch using the ANSYS Design Modeler software. In all, about six parameters are singled out, of which three parameters have continuous range and three are scalar numbers (Fig. 9).



Parameter	Name	Range
P1	Length 1	Nominal \pm 30%
P2	Width	Nominal \pm 20%
P3	Length 2	Nominal \pm 25%
P4	Supports	Nominal \pm 3
P5	Clamp 1	Nominal \pm 1
P6	Clamp 2	Nominal \pm 1

Fig. 9: Parameters and their range for seal profile optimization (reference model)

Gasket Modelling

Seal is modeled as gasket with INTER195 elements having eight nodes and three translation degrees of freedom at each node. Considering the actual seal profile in the housing model for simulation results in element distortion with unusually long run times, rendering is infeasible. Hence gasket modeling is always more reliable, with swift turn-around times in parametric study. Closure versus pressure curve is obtained from sectional analysis carried out on the optimized seal profile (Fig. 10).

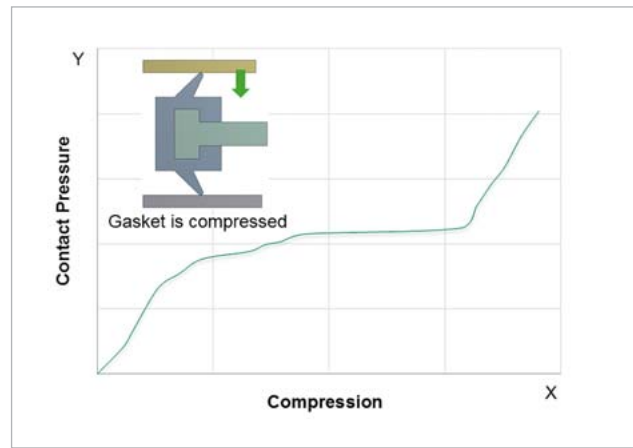


Fig. 10: Closure versus pressure curve (reference model)

Boundary Condition

Boundary condition for static analysis is imposed by fixing the housing and applying bolt torque at the clamp/hinge location. Normal gasket compression and pressure is considered as output from the analysis. When closely observed (Fig. 11), gasket compression and gasket pressure is adequate along the periphery but lower in the bridge region that is region responsible for separating the clean and dirt sides of the filter. Hence pressure in bridge region is of paramount importance, because it directly dictates the sealing efficiency of the whole filter.

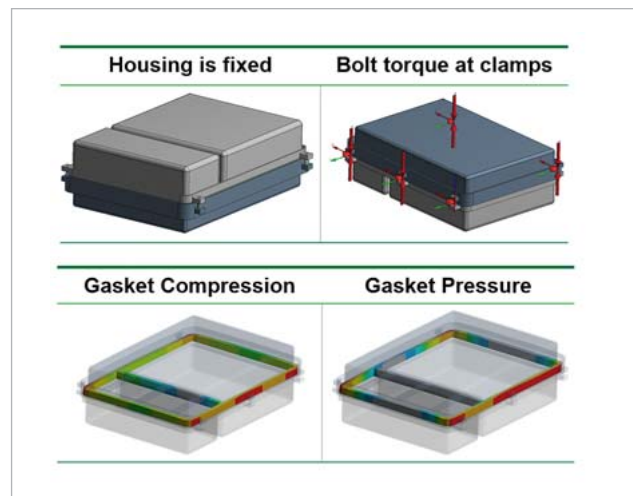


Fig. 11: Boundary conditions, gasket compression and gasket pressure

Sensitivity Analysis

The sensitivity analysis is executed within the given range of the parameters until CoP attains a stable value. Width and length2 are the influencing parameters in determining gasket pressure at the bridge region (Fig. 12, see next page). The pressure distribution graph (Fig. 13, see next page) aids designers in estimating the behavior of pressure distribution for a similar kind of model, hence enhancing the product design very early in the initial phase.

Gasket Pressure Distribution in bridge region

The background color (Fig. 13) represents the gasket pressure distribution in bridge region, while the major influencing parameters, width and length2 are X and Y axis respectively. Isoline represents minimum required pressure at the bridge region and is set as per the design specification. In this case, as a reference, it is set to 100 mbar. To meet the required contact pressure, X and Y coordinates, lying on the left of the line, are to be chosen. The X and Y coordinates in the upper right corner of the plot indicate the low pressure region.

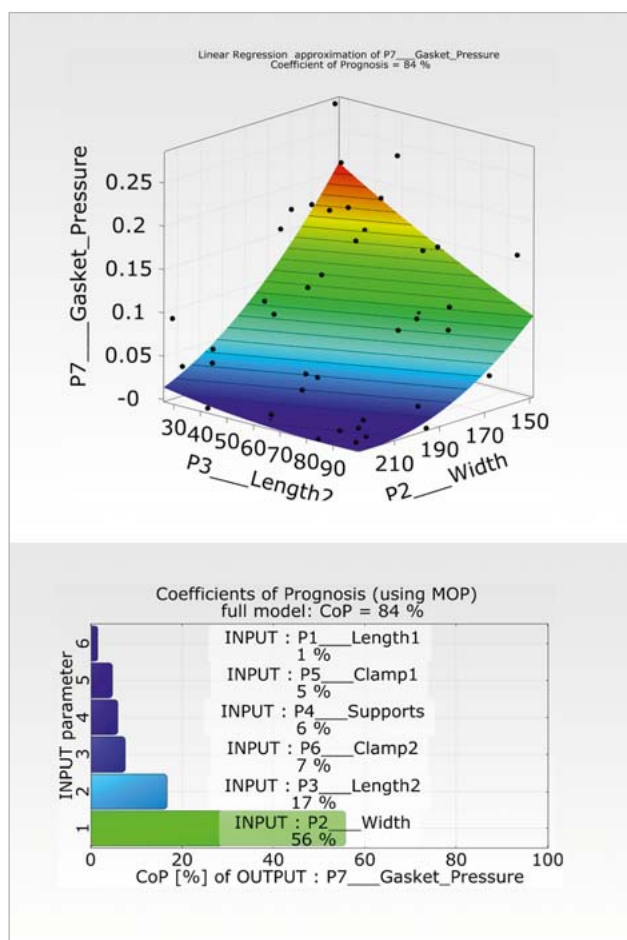


Fig. 12: MOP and CoP for gasket pressure

Excel MOP

In addition to pressure distribution plot, the excel MOP is handed over to the designers in order to derive the exact value of pressure with changes in the input parameter (Fig. 14). To start with, the MOP solver has to be installed in excel and then input parameters can be varied within the advised range. Afterward, the *.bin file obtained from sensitivity analysis is loaded into the MOP solver and initiated. Since the behavior of results outside of the range cannot be predicted, extrapolation is discouraged.

Conclusion

- Simulation coupled with statistics is employed early in the design phase of an air filter. This raises the bar as a

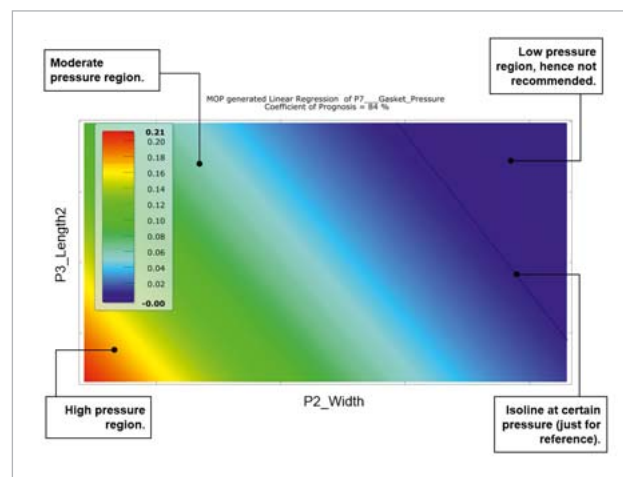


Fig. 13: Pressure distribution on bridge region

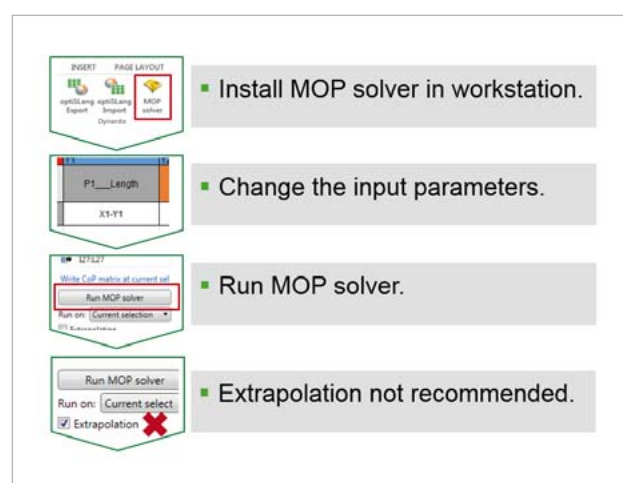


Fig. 14: Steps to use excel MOP

classic example of simulation driven product development project resulting in reduced lead time, increased quality and reduced development costs.

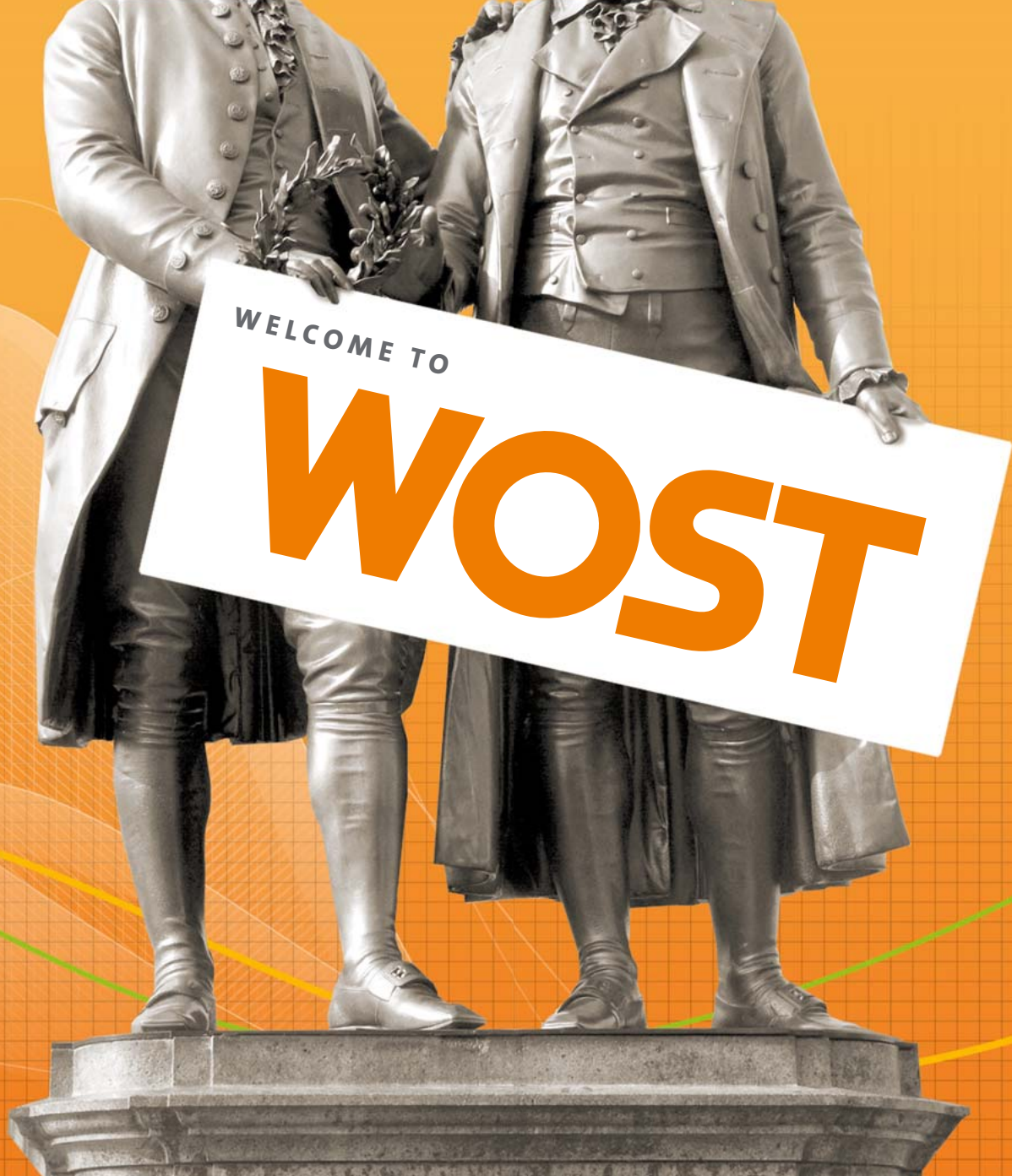
- Gasket volume is lowered by 13 % for the same mounting force and contact pressure, leading to savings in material
- Width and length2 are the influencing parameters on gasket pressure in the bridge region. Optimization of the complete assembly further enhances the performance of the air filter.
- Combined effect of optimizing the housing and profile may yield an optimized assembly and serve as an outlook of the current studies.

Author

Prashant Mugabasav (MANN+HUMMEL)

Acknowledgement

I would like to thank and acknowledge my colleagues, Mr. Kaushik Iyer, Mr. Mridul Sharma, Mr. Vijayendran and Mr. Shajahan along with support from center of competence, Dr. Florian Keller and Mr. Sven Epli.



ANNUAL WEIMAR OPTIMIZATION AND STOCHASTIC DAYS

Your conference for CAE-based parametric optimization, stochastic analysis and Robust Design Optimization in virtual product development.

The annual conference aims at promoting successful applications of parametric optimization and CAE-based stochastic analysis in virtual product design. The conference offers focused information and training in practical seminars and interdisciplinary lectures. Users can talk about their experiences in parametric optimization, service providers present their new developments and scientific research institutions inform about state-of-the-art RDO methodology.

Take the opportunity to obtain and exchange knowledge with recognized experts from science and industry.

You will find more information and current dates at:
www.dynardo.de/en/wosd.

We are looking forward to welcoming you to the next Weimar Optimization and Stochastic Days.

Contact & Distributors

Worldwide

Dynardo GmbH
Steubenstraße 25
99423 Weimar
Phone: +49 (0)3643 9008-30
Fax.: +49 (0)3643 9008-39
www.dynardo.de
contact@dynardo.de

Dynardo Austria GmbH
Office Vienna
Wagenseilgasse 14
1120 Vienna
www.dynardo.at
contact@dynardo.at

Worldwide distribution of ANSYS optiSLang

ANSYS, Inc.
Canonsburg
www.ansys.com

Worldwide distribution of optiSLang

LightTrans GmbH
Jena
www.lighttrans.de

Germany

CADFEM GmbH
Grafing b. München
www.cadfem.de

Austria

CADFEM (Austria) GmbH
Vienna
www.cadfem.at

Switzerland

CADFEM (Suisse) AG
Aadorf
www.cadfem.ch

Czech Republic, Slovakia, Hungary

SVS FEM s.r.o.
Brno-Židenice
www.svsfem.cz

Sweden, Denmark, Finland, Norway

EDR & Medeso AB
Västerås
www.edrmedeso.com

United Kingdom of Great Britain and Northern Ireland

CADFEM UK CAE Ltd
Croydon, Surrey
www.cadfemukandireland.com

Ireland

CADFEM Ireland Ltd
Dublin
www.cadfemukandireland.com

Turkey

FIGES A.S.
Istanbul
www.figes.com.tr

North Africa

CADFEM Afrique du Nord s.a.r.l.
Sousse
www.cadfem-an.com

Russia

CADFEM CIS
Moscow
www.cadfem-cis.ru

India

CADFEM Engineering Services India
Hyderabad
www.cadfem.in

USA

CADFEM Americas, Inc.
Farmington Hills, MI
www.cadfem-americas.com

Ozen Engineering Inc.
Sunnyvale, CA
www.ozeninc.com

USA/Canada

SimuTech Group Inc.
Rochester, NY
www.simutechgroup.com

Japan

TECOSIM Japan Limited
Saitama
www.tecosim.co.jp

Korea

TaeSung S&E Inc.
Seoul
www.tsne.co.kr

China

PERA-CADFEM Consulting Inc.
Beijing
www.peraglobal.com

Publication details

Publisher

Dynardo GmbH
Steubenstraße 25
99423 Weimar
www.dynardo.de
contact@dynardo.de

Executive Editor & Layout

Henning Schwarz
henning.schwarz@dynardo.de

Registration

Local court Jena: HRB 111784

VAT Registration Number

DE 214626029

Publication

worldwide

© Images

Cover image & p. 2: Boeing 747-8 © Lufthansa

Copyright

© Dynardo GmbH. All rights reserved
The Dynardo GmbH does not guarantee or warrant accuracy or completeness of the material contained in this publication.